

UC Berkeley

Consortium on Deburring and Edge Finishing

Title

An Experimental Investigation on the Influence of Process Parameters During Chip Formation

Permalink

<https://escholarship.org/uc/item/1m17m8xh>

Author

Reich-Weiser, Corinne

Publication Date

2006-05-01

**An Experimental Investigation on the Influence of Process Parameters
During Chip Formation**

by

Corinne Lee Reich-Weiser

B.S. (University of California at Berkeley) 2003

A report submitted in partial satisfaction of the
requirements for the degree of
Masters of Science, Plan II

in

Mechanical Engineering

in the

GRADUATE DIVISION

of the

UNIVERSITY OF CALIFORNIA, BERKELEY

Committee in charge:
Professor David Dornfeld, Chair
Professor Sara McMains

Fall 2006

Abstract

As machines and products increase in productivity while shrinking in size, issues of contamination related failures become a greater risk. Previously, common contaminants such as sand from sand casting, dust from the air, or chips from machining, were within generally allowable product tolerances. The semiconductor industry was first to encounter contamination related problems from dust on their micro sized features. Now, the automotive industry is discovering millimeter sized chips blocking lubrication valves and scoring precision surfaces. This report details an experimental investigation of how chip related contamination may be controlled by varying milling and drilling cutting parameters such as feed, speed, depth of cut, and lubrication. Based on the assumptions of this paper, where the optimal chip is likely short, lightweight, with a large wavelength, and few rotations, it is found that the optimal milling chip is produced with increased speed, increased lubrication, decreased feed, and decreased depth of cut. For drilling, the optimal chip is accomplished through increased lubrication, decreased speed, and increased feed. Future research is required to determine the optimal chip type.

Contents

List of Figures	iii
List of Tables	v
1 Introduction	1
1.1 Design Rules for Cleanliness (Level I)	2
1.2 Chip and Burr Control and Cleanability (Levels II & III)	4
1.2.1 Burr and Process Relationship	5
1.2.2 Chip and Process Relationship - Basics of Chip Formation	8
1.2.3 Cleanability of Chip Types	9
1.3 Cleanliness in the Automotive Industry (Level IV)	9
1.4 Environmental Considerations	10
1.5 Research Objectives	11
2 Chip Formation Literature Review	12
2.1 Chip Formation	12
2.2 Temperatures	15
2.3 Cutting Forces	16
2.4 Chip Flow and Geometry	17
2.5 Chip Classification	24
2.6 Chip Breaking & Control	26
2.7 Finite Element Prediction	27
3 Experimental Procedure	30
3.1 Chip Production and Collection	31
3.2 Chip Classification - Separation of Chips by Type	33
3.3 Chip Measurement	36
3.4 Design of Experiments	39
3.5 Correlation	40
3.6 Analysis of Variance using Matlab	41

4	Experimental Results and Analysis	43
4.1	Milling	44
4.2	Drilling	52
4.3	Chip and Burr Control	58
5	Conclusions	61
5.1	Summary	61
5.2	Future Work	62
	Bibliography	64
A	Graphs of Milling Correlations & Effects	69
B	Graphs of Drilling Correlations & Effects	78

List of Figures

1.1	Four levels of design and manufacturing.	3
1.2	Edge effect on burr formation and optimizing geometry for water jet access	4
1.3	Flowchart of research objectives	5
1.4	Drilling burr control charts	6
1.5	Exit order sequence illustration	7
1.6	Web-based drilling burr control chart for predicting likely burr formation.	8
1.7	Milling chip lodged in a water jacket passageway and an oil valve.	10
2.1	Segmented chip formation	14
2.2	Progression of chip formation as tool velocity increases	14
2.3	Regions of heat formation during machining	16
2.4	Experimental results for the temperature rise with cutting velocity of three materials	16
2.5	Measured cutting forces for three machined steels	18
2.6	Measured cutting forces for five heat treatments of high carbon mold steel	18
2.7	Merchant force circle	20
2.8	Chip flow diagram.	20
2.9	Computer generated chip geometries showing effect of lateral curl	21
2.10	Chip curl in iron for dry and lubricated machining	22
2.11	ISO 3685 chip classification.	25
2.12	Images of continuous, serrated, discontinuous, and built-up edge chips	26
2.13	Sample chip breaking control chart	28
2.14	Simulation illustrating effect of lubrication on chip curl	29
3.1	Important milling angles	33
3.2	Photographs of milling cutter	33
3.3	New drill specifications	34
3.4	Photograph of the work drill cutting edge.	34
3.5	Experimental collection of machining chips.	34
3.6	Drilling and milling chips sorted by size and shape.	35
3.7	Drilling chip classification	35
3.8	Milling chip classification	36

3.9	ISO chip classification with dominant curl mechanism added.	37
3.10	Up and side curl illustration for milling.	37
3.11	Chip geometry measurements	38
A.1	Effect of process parameters on chip weight for milling	70
A.2	Effect of process parameters on chip width for milling	71
A.3	Effect of process parameters on chip wavelength for milling	72
A.4	Effect of process parameters on chip shear zone wavelength for milling	72
A.5	Effect of process parameters on chip shear zone height for milling	72
A.6	Effect of process parameters on chip shear zone height divided by the feed for milling	73
A.7	Effect of process parameters on chip edge thickness divided by the feed for milling	73
A.8	Effect of process parameters on chip rotations for milling	74
A.9	Effect of process parameters on the chip minimum diameter for milling	75
A.10	Effect of process parameters on the chip maximum diameter for milling	76
A.11	Effect of process parameters on the chip length for milling	77
B.1	Effect of process parameters on the chip width for drilling	79
B.2	Effect of process parameters on the chip width for drilling	80
B.3	Effect of process parameters on the chip weight for drilling	81
B.4	Effect of process parameters on the chip rotations for drilling	82
B.5	Effect of process parameters on the chip maximum diameter for drilling	83
B.6	Effect of process parameters on the chip maximum diameter for drilling	84
B.7	Effect of process parameters on the chip wavelength for drilling	85
B.8	Effect of process parameters on the chip shear zone wavelength for drilling	86
B.9	Effect of process parameters on the chip shear zone height for drilling	87
B.10	Effect of process parameters on the chip shear zone height divided by the feed for drilling	88

List of Tables

3.1	Milling experiments	32
3.2	Drilling experiments.	32
4.1	Milling correlations. Significant values are boxed.	45
4.2	Milling effects: average change in output value when going from low to high input value. Largest effects are boxed	46
4.3	Milling p-values: significance of relationship between variables and measured parameters. Significant p-values are boxed.	47
4.4	Photos of typical milling experimental outputs.	53
4.5	Drilling correlations.	54
4.6	Drilling effects: average change in output value when going from low to high input value. Largest effects are boxed.	55
4.7	Drilling P-Values: a value below 0.01 indicates the relationship is significant.	56
4.8	Photos of drilling experimental results.	59

Acknowledgments

This research would not be possible without the ongoing support and guidance of my advisor, Professor David Dornfeld, and the Laboratory for Manufacturing and Sustainability at UC Berkeley. Thank you to Daimler Chrysler and Klaus Berger for providing the motivation, opportunity, and resources to conduct this research. Thank you also to Professor Sara McMains, Miguel Avila, Shantanu Tripathi, Jeffrey Hartnett, and Jonathan Iloreta for their insights and advice.

Chapter 1

Introduction

Trends in technology are towards smaller, faster, and more reliable goods. This applies in all sectors, including automotive and aerospace. But as parts become smaller, issues of precision and tolerance become more important. For example, a micro gear with teeth that are 10 microns in length, cannot tolerate a commonly stellar precision of the same magnitude. This also applies for contamination on the part. It was once the case that a small chip from the machining process or a piece of sand left over from casting was negligible; however these are now fatal to the part's functionality and reliability. In the automotive industry, cleaning of complex mechanical components can comprise 8-20% of the manufacturing costs [1].

There are four key stages of product development that fundamentally affect the product's appearance and functionality. These are considered the four levels of design (Figure 1.1). In level I, the product is conceptualized and prototyped; decisions at this level affect every following level. Following design, level II involves decisions on how to

manufacture the product. If the designers at level I considered manufacturing issues, then level II should be relatively simple; but, design for manufacturing is only one of many considerations made by the level I designers. Level III occurs after manufacturing has begun; small changes may be made to the system, however these changes are very limited and must fit with the tooling and layout put in place at level II. With the completion of manufacture, parts are often deburred and cleaned to avoid sharp hazardous edges, ensure proper mating of parts, and improve aesthetics; this is level IV.

New research presented in this report concerns minimizing the amount of cleaning required in level IV by optimizing the process parameters (cutting tools, cutting speeds, lubrication) put in place during levels II and III. This discussion includes a brief review of previous knowledge on burr and chip formation, design rules for cleanability, and details about new research on controlling chip geometry for cleanability. Ultimately, knowledge gained about levels II, III, or IV should be used in level I to design a part that is most easily manufactured, cleaned, and deburred.

1.1 Design Rules for Cleanliness (Level I)

At the beginning stage of creating a new product, all aspects of its design are in consideration. Design for cleanability provides rules of thumb for a designer to ensure that the final part will be easily cleaned both after it is manufactured and during its life. A lot is known about designing parts so that burr formation is minimized; however, design for cleanability is a relatively new field. Sipitkowski [2] has written a series of articles on design for cleanability including ideas on keeping parts simple, allowing for fast drying and

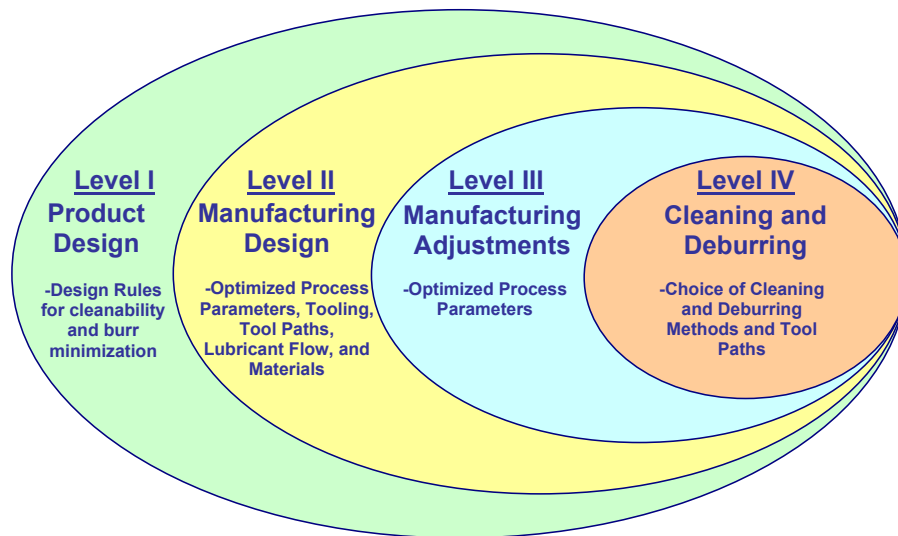


Figure 1.1: Four levels of design and manufacturing.

rinsing, and ensuring there are few dead end passageways in the part (i.e. use through holes rather than blind holes). He also recommends including draft angles on the part to allow fast drainage, which agrees with the basic rule of minimizing burr formation by ensuring the part has no corners less than 90 degrees (figure 1.2a). Sand casting is also not recommended [3], because the rough edges hinder part washing and drying time. Ironically, most engine parts that have a problem with cleanliness, due to complex and narrow passageways, are made with sand casting. Some rules for cleaning parts with water jets are being developed, which would allow the designer to understand how his or her designs will affect subsequent cleaning operations. Figure 1.2b illustrates issues of accessibility for cleaning passageways with water jets.

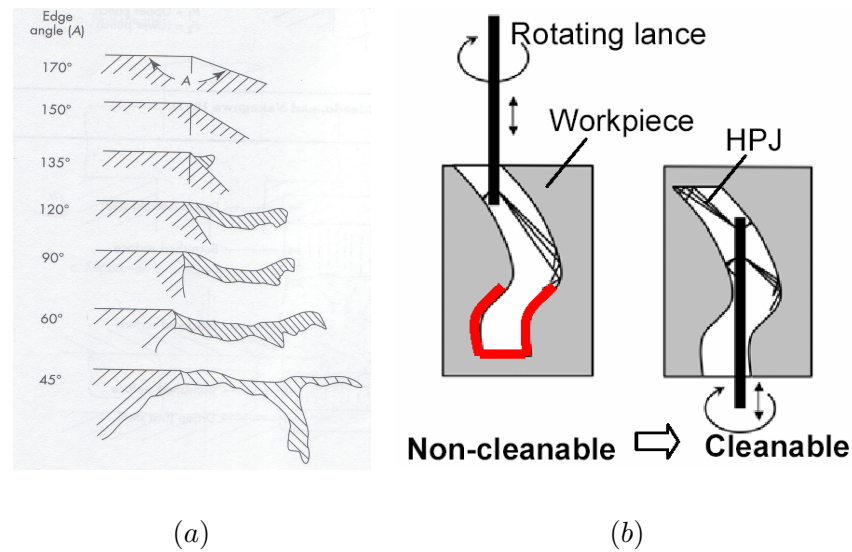


Figure 1.2: (a) edge angle effect on burr formation [4], (b) optimizing part geometry to allow access by water jet lances [5].

1.2 Chip and Burr Control and Cleanability (Levels II & III)

Figure 1.3 shows three research areas necessary to understand how to optimize both burr and chip formation (in levels II and III) for part cleanability. This neglects how part design (level I) plays a role in minimizing burr formation, and focuses on the cutting processes.

A great deal of work has been done on controlling and understanding burr formation to minimize or even eliminate deburring as a finishing process [6, 4]. Chip formation has also been extensively studied, but not from the perspective of chips as a contaminant. Finally, understanding what chip types are more or less a problem for cleanliness is a topic for future research. When these three research areas are complete, design rules for levels II will be in place for optimal part cleanliness.

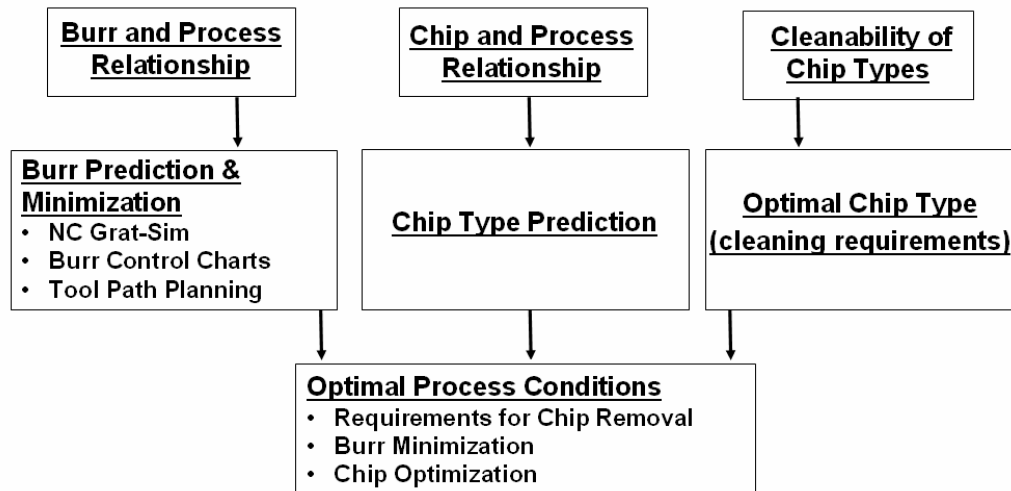


Figure 1.3: Flowchart of research objectives (levels II and III).

1.2.1 Burr and Process Relationship

Important work on burr formation and minimization (size, location, shape, etc.) has been done by Dornfeld and his research group [5] and others [4]. This work was motivated by the many problems caused by burrs during manufacturing: 2% to 8% of costs during mechanical cutting are caused by burrs; sharp edges and burrs cause injuries during handling; and burr formation has been linked to excessive tool wear [7].

Burr formation can be minimized by understanding and controlling certain influential process conditions such as feed, speed, tool geometry, workpiece orientation, and workpiece material properties. A database of burr size measurements obtained while adjusting these parameters provides the basis for a burr control chart. For milling, the exit angle from the part is most influential in burr formation. For drilling, the tool geometry and orientation with respect to exit surface has been shown significant to burr formation

[6].

As an example, Figure 1.4 shows typical burr control charts for drilling stainless and low alloy steels; the burrs were formed by drilling with a split point twist drill. Useful for all materials of the same type (carbon steel, for example), and normalized to cover a range of drill diameters, these charts provide information on what range of process parameters should be used to optimally minimize burr formation. This chart predicts the approximate boundary between three standard burr types; small uniform burr (type I), large uniform burr (type II), and crown burr (type III). The burr height scales with distance from the origin, and the grey box indicates common recommended process parameters for this material.

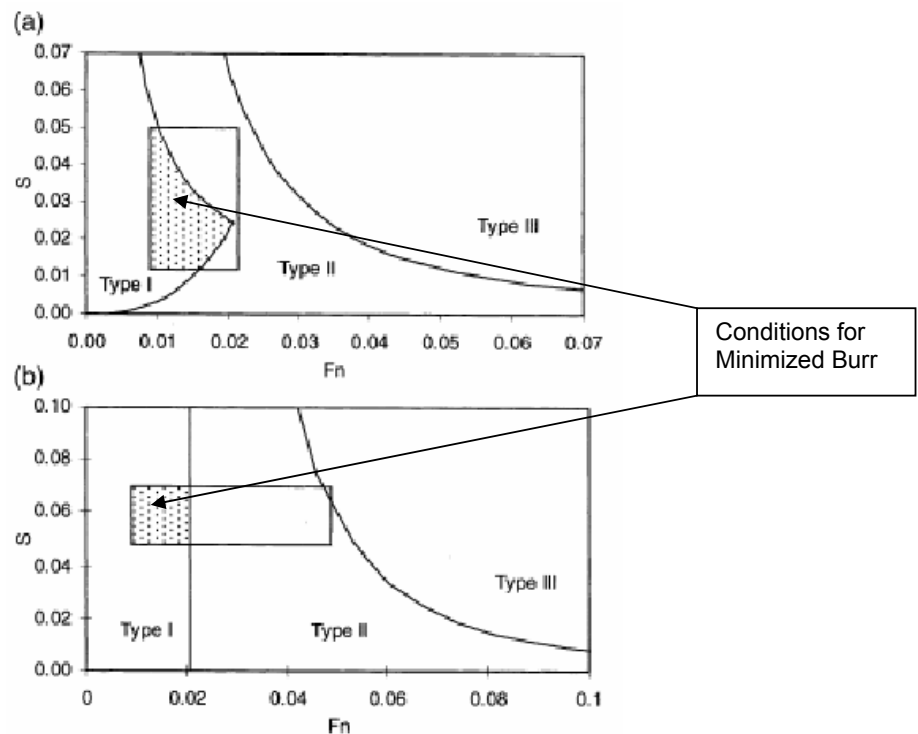


Figure 1.4: Drilling burr control chart for (a) stainless steel (AISI 304L) and (b) low alloy steel (AISI 4118), where S is the spindle speed [rpm] and F_n is the normalized feed (feed [mm/rev] divided by drill diameter) [5].

Additionally, burr formation during milling is heavily influenced by the tool's orientation with respect to the workpiece. This knowledge is reflected in the Exit Order Sequence, Exit Angle, and Tool Path Planning work done by Dornfeld and co-workers. If the exit angle (i.e. the velocity angle of the cutter with respect to the workpiece edge) is below a critical value for the workpiece material, then the burr is minimized [8]. Shown in Figure 1.5, the exit order sequence determines if the material is cut or bent over leaving a burr that may be as large as the depth of cut. Sequence CBA is most likely to leave a large burr.

Burr databases such as the burr control chart are being integrated with an internet-based expert system to provide interactive and timely results for today's industry problems. An example of this is shown in Figure 1.6, where the process parameters are supplied as input, and the predicted burr is represented as a red dot on the control chart.

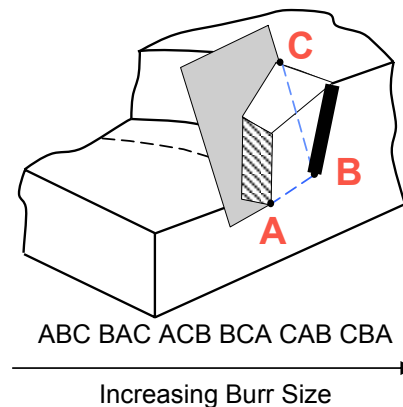


Figure 1.5: Exit order sequence. Shown here is sequence ABC [8].

The first stage of this burr expert website includes modules and case studies from UC Berkeley's short course on burr minimization. It also provides a forum for members to

exchange ideas and technology discoveries, thus enabling users a fast and effective source of data and insights from a wide population of people with similar problems [5].

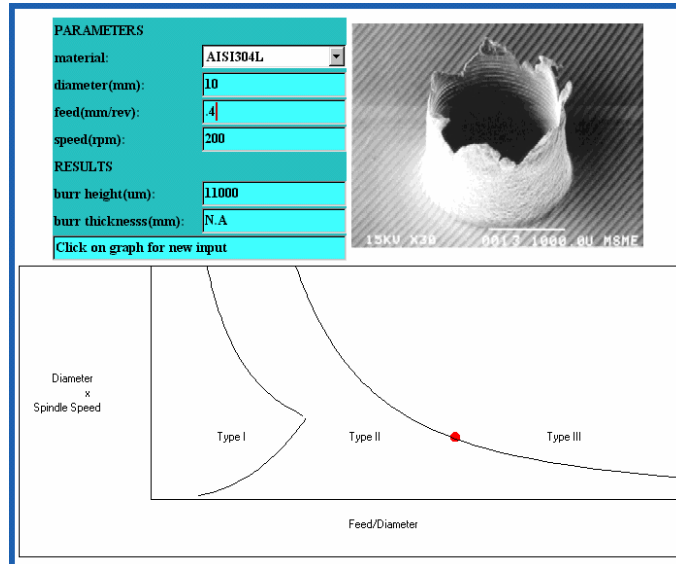


Figure 1.6: Web-based drilling burr control chart for predicting likely burr formation.

1.2.2 Chip and Process Relationship - Basics of Chip Formation

Prior research on chip formation during both Milling & Drilling is discussed in chapter 2. Researchers have sought to understand various material removal processes through both theoretical models and experiment. The primary focus of prior research has been chip breaking, cutting forces, and surface quality. For example, many papers concern breaking the chip so it may be more easily moved away from the machining area to facilitate further machining. The “efficiency of a cutting process depends on having small manageable chips” [9]. Further work is needed to understand chip formation as it relates to cleanability.

1.2.3 Cleanability of Chip Types

It is the subject of additional research to determine exactly what it means to create a cleanable chip, but most would agree it is relative to chip size, shape, and material properties. Some additional guesses as to the optimal chip geometry are as follows:

1. The largest dimension across the chip should be smaller than the smallest internal dimension of the workpiece. This avoids chips from being firmly lodged within a narrow passageway.
2. Chips that are very curly or long should be avoided or risk being entangled within the part or with each other.
3. Thin or brittle chips may be more easily broken and removed.
4. Heavier chips may be more difficult to wash away with flowing water.
5. Chips with a larger surface area have increased drag and may wash away more easily.
6. The chip's ideal shear zone height may be large or small: large to induce discontinuous chip formation, which ensures smaller chips, or small to reduce the likelihood of chips snagging on side walls or with each other.

1.3 Cleanliness in the Automotive Industry (Level IV)

As the tolerances required for mechanical instruments become increasingly small, the requirements for contamination become more stringent. In a passageway that must be

2 microns in diameter, a small chip remaining from a machining operation can be detrimental to the part's function.

Specifically, the research conducted in this paper is geared towards the problems of cleanliness associated with the cylinder head of internal combustion engines. These components are currently cleaned in a variety of inefficient ways, such as ultrasound to loosen chips and blasting with waterjets from all directions. However, these parts contain an intricate maze of water and oil channels for cooling and lubrication purposes, and once a machining chip has traveled into the maze during manufacturing, it becomes a challenge to remove. This is often due to the chip becoming lodged like a spring or finding itself at the dead end of a passageway. However, these often release days or months into the use phase, causing premature failure. Figure 1.7 shows a chip that was found lodged deep in a water channel and a chip found lodged in the valve that controls oil flow. Here the chip is blocking the valve's ability to close completely.



Figure 1.7: Milling chip lodged in a water jacket passageway and an oil valve.

1.4 Environmental Considerations

The current method of cleaning, water jets, is inefficient and wasteful. It is often done by shooting water at the part externally, without entering the part, and it fails to

penetrate and clean the deeper passageways. Fluid flow in the cylinder head is a major problem for cleanability, because the fluid loses its energy as it rounds the many corners and hits dead ends.

Additionally, machining is often done with large quantities of coolant, which is hazardous to the environment and the workers [10]. By understanding how to better design parts and the manufacturing process to minimize contamination and make cleaning easier, both the environment and the manufacturer's bottom line will benefit.

1.5 Research Objectives

This thesis, on how chip geometry may be manipulated by varying key process parameters, is motivated by the growing problem of part cleanliness. It is hoped that by understanding and controlling the chip form, only chips that are more easily cleaned from the part will be produced. The first step is to observe how parameters such as feed, speed, and depth of cut affect aspects of the final chip's morphology such as size, weight, and degree of straightness.

The previous research on chip formation is extremely in depth and detailed; however, the lack of focus on cleanability leaves it incomplete. In this paper chip formation and prediction is investigated with the interest of part cleanliness in mind. Thus, the measured aspects considered important about each chip were those thought to directly affect a chip's likelihood of being caught in a part, as was discussed previously. Additionally, this research is not looking at individual chips produced by a closely controlled experiment, but at the general results seen in industry.

Chapter 2

Chip Formation Literature Review

A brief review of the research conducted over the past century is included here as it is relevant to the topic of how particular machining parameters may affect chip formation. First, the topic of forces, temperatures, and chip flow are discussed, because understanding the chip's formation is crucial to controlling it and chip flow research was the starting point of chip research over a century ago. With this understanding, additional research on breaking and controlling the chips is covered, followed by a discussion of previous methods used to classify chips; the importance of a common language to describe chips is crucial to comparative work. Finally, predictive work using finite element analysis is reviewed.

2.1 Chip Formation

A highly debated topic, the mechanism for chip formation is attributed to either shear localized deformation within the chip (dynamic re-crystallization or a phase change) or brittle fracture. The confusion arises because at extremely low cutting speeds, a segmented

chip like that seen at high speeds is known to be caused by brittle fracture within the shear plane; however, at high speeds, a metallurgical investigation of the segmented chip reveals no brittle fracture [11]. Despite the evidence, some authors argue there is not the required reduction in forces seen at the transition from continuous to segmented chip formation to account for the plastic deformation and dynamic re-crystallization that is predicted by the adiabatic shear model. These opponents of adiabatic shear also comment that there is not enough time for the material to be significantly softened as it passes through the high temperature shear zone [12].

Segmented chip formation, however, is most likely the result of deformation rather than fracture within the chip. This type of deformation is referred to as adiabatic or shear localized slip, and it occurs when the local temperature increase (heat from plastic deformation in the shear plane) causes a decrease in strength greater than the increase from strain hardening [11]. As seen in Figure 2.1, the region of intense shear, extending through the chip from the tool tip, will start to deform and rotate counterclockwise due to “stick” between the chip and tool face. At some critical shear, the two chip segments will slide past each other, and the material will slip past the tool face. The cyclic chip velocity predicted by adiabatic slip has been observed using high speed photography [11], providing further evidence for this mechanism.

It is known that the transition to segmented chip formation (illustrated in Figure 2.2) will occur at lower speeds for materials with high hardness and low diffusivity [13]. This information favors well for the adiabatic slip model, because lower diffusivity materials will not efficiently conduct away the heat formed in the shear plane, which will result in

catastrophic shear at lower velocities. Indeed, it seems the trend of high hardness with quick formation of discontinuous chips favors the fracture method of formation; however, this trend also matches with adiabatic slip because it implies the material will not be able to flow past the tool, and is more likely to stick (and consequently slip) at the tool-chip interface. The distance between these shear zones has been shown experimentally to increase with cutting speed [14].

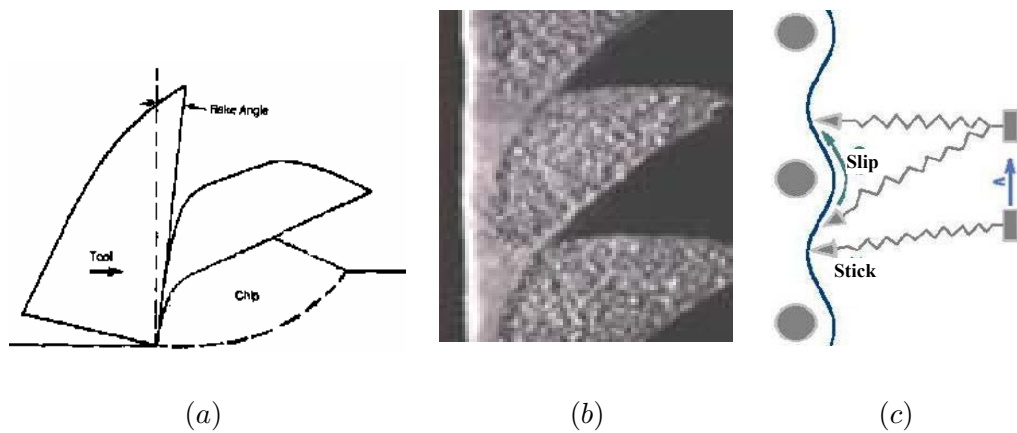


Figure 2.1: (a) Illustration of segmented chip formation where the dashed line indicated the region of intense shear deformation [11], (b) micrograph of segmented chip formed in hardened steel at 4.3m/s [14], and (c) schematic of stick slip phenomenon at the atomic scale as the chip flows past the tool face [15].

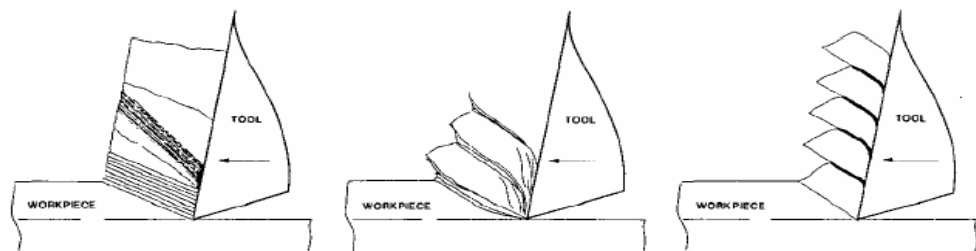


Figure 2.2: The progression of chip formation from continuous shear to localized adiabatic shear as the tool velocity increases into the high speed regime [11].

2.2 Temperatures

There are three sources of heat generation during a machining operation: deformation within the shear zone; friction along the tool-chip interface (as seen in Figure 2.3); and for a tool that has a rounded tip, friction along the clearance face of the tool, which leads to rake wear.

As the tool velocity increases, the rate of heat generation rises above the material's rate of thermal diffusivity, causing a temperature rise. This continues until a critical velocity is reached where the workpiece reaches its melt temperature; from this point on the temperature no longer increases. This phenomenon is reported by Flom [11] recounting Polosatkin & Titov's experiments, which demonstrated a rising tool temperature in cutting steel up to a peak at around 11,000 m/min, where the melting point of the work material was reached. They observed no further change in the cutting steel's temperature up to 44,000 m/min. They weren't the only ones to see this trend; Figure 2.4 shows recent results of temperatures leveling out with increasing tool velocity (note that in this case the peak temperatures recorded for each material are slightly less than the melt temperature because the recording is taken from the backside of the chip rather than the interface), making clear the importance of material diffusivity to rate of temperature increase.

In light of these observations, along with some physical intuition, a previous proposal by Salomon that the temperature would drop with increasing velocity [16] seems unlikely. If, in fact, the temperature does begin to drop, due to the decreased friction and shear of cutting a melted material, then as soon as the temperature drops below the melting temperature, the friction and shear should rise to once again melt the material. If careful

measurements are taken of the workpiece in these ultra high speed zones, it is likely a cyclic pattern would be found about the mean melt temperature.

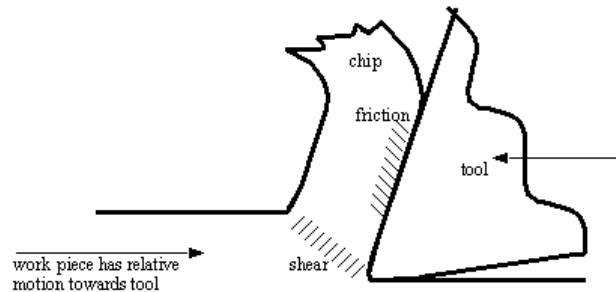


Figure 2.3: Regions of heat formation during machining [17].

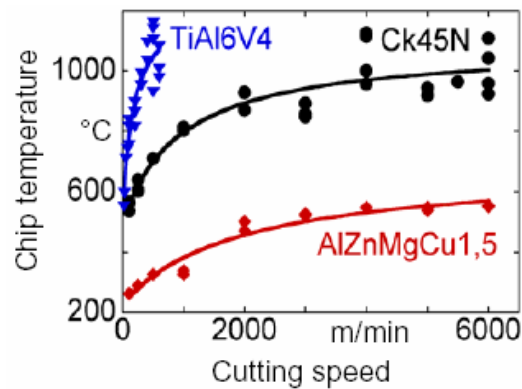


Figure 2.4: Experimental results for the temperature rise with cutting velocity of three materials: Titanium Alloy (blue, low thermal diffusivity) and Carbon Steel (black), feed = 0.1mm, depth of cut = 1mm; and Aluminum Alloy (red, high thermal diffusivity), feed = 0.25mm, depth of cut = 2mm [18].

2.3 Cutting Forces

When the velocity increases, so does the temperature and degree of adiabatic shear. How does this affect the cutting forces? They decrease. An initial swell in force is sometimes seen due to strain hardening; however, rising temperatures eventually override

strain hardening and weaken the material so it can “flow” past the tool with ease. But the story quickly changes at high speeds when the inertial effects of the chip changing direction at the tool begin to dominate; the assumption is then that the forces rise. Force measurements in the very high speed regime are not easily obtained, however once the cutting speed increases past 4000 m/min the start of an upward trend can be seen in Figure 2.5.

Material hardness is an important factor in how quickly the cutting forces will drop. As shown in Figure 2.6, the hardest material initially undergoes a much greater cutting force, but as the velocity increases, and shear localized chip formation becomes the dominant factor, this force quickly drops to almost equal that of the more ductile material’s cutting forces.

As with chip velocity, when the cutting conditions are fixed, the measured friction force during high speed machining is cyclic [19]. Clearly, the link here is a high friction force when the chip “sticks” and a low friction force when the chip “slips.”

2.4 Chip Flow and Geometry

Basic analysis of cutting processes started in the late 1800’s with the work of Tresca and Mallock who first pointed out two important elements of metal cutting: friction between the tool and workpiece, and plasticity [22]. More than half a century later, a simple model of orthogonal cutting was created by Merchant, which argued that the shear angle would occur in a location to minimize energy usage during cutting. This work provided the starting point for additional research on machining, and started researchers thinking about

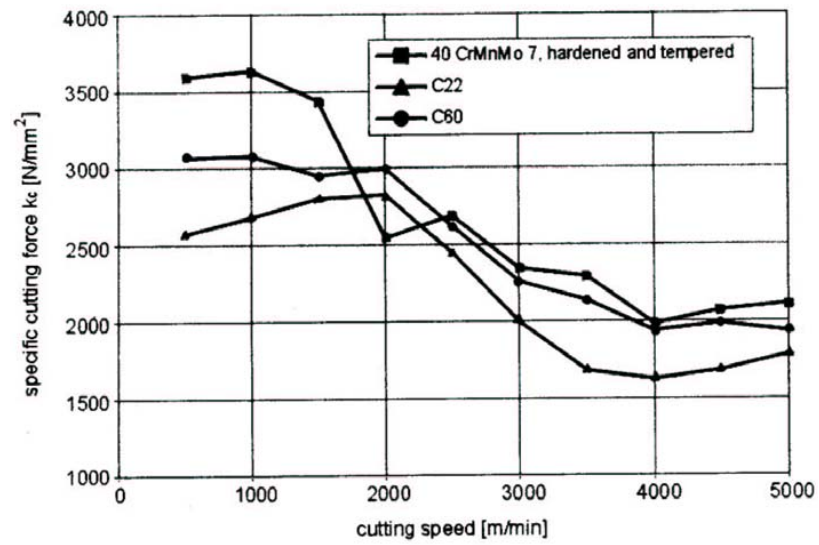


Figure 2.5: Measured cutting forces for three machined steels [20]

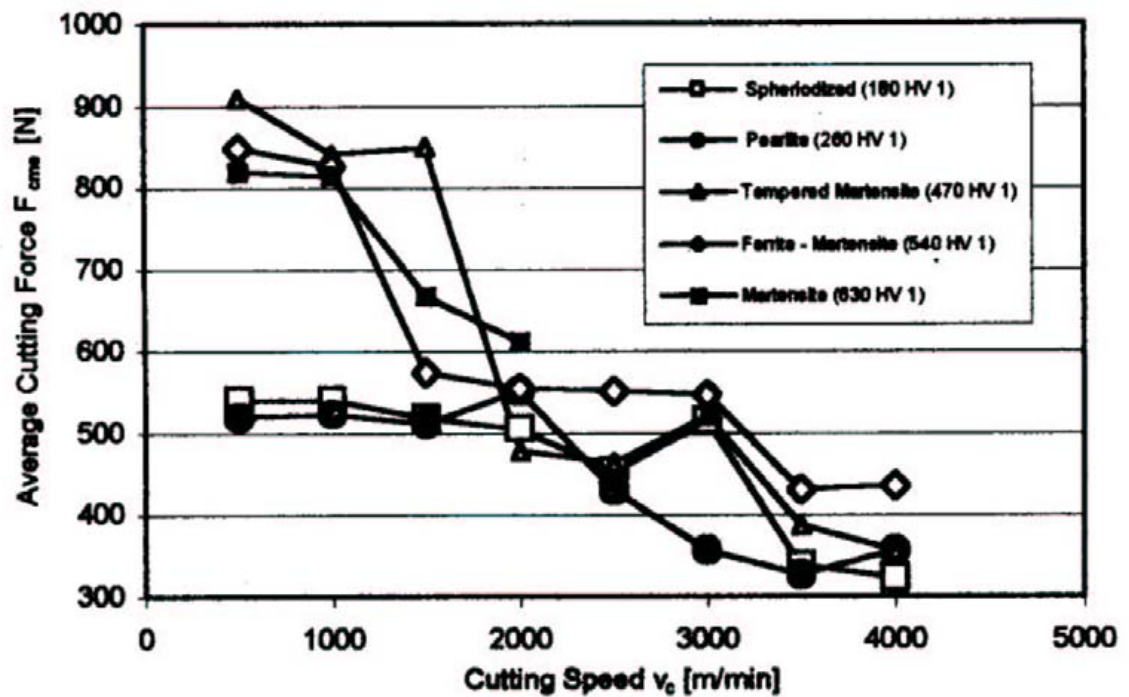


Figure 2.6: Measured cutting forces for five heat treatments of high carbon mold steel (40CrMnMo7). A higher initial cutting force indicates a higher material hardness [21].

the energy involved with shearing along the shear plane, friction, and cutting forces. For additional modeling accuracy, future researchers added a secondary shear zone along the tool rake face.

By balancing the forces in Merchant's model (Figure 2.7), it can be determined that decreasing the rake angle or increasing friction will decrease the shear angle, resulting in a thicker chip [23]. Kalpakjian goes on to state that increasing friction, by removing lubricant between the tool and workpiece, will cause a shear strain increase from the reduced shear angle, making a built up edge more likely, causing the total energy to increase, increasing the temperature generation, and reducing surface quality.

These predictions match the experimental results of Kishawy [24], who demonstrated that the chip thickness may be increased by increasing the tool wear (i.e. decreased rake angle) or increasing the cutting speed (i.e. increased friction). He also mentioned that lubrication minimized this effect. Jawahir *et al.* [25] argued the affects of greater cutting speed are decreased force, decreased secondary shear zone thickness, and decreased temperature.

In 1993, an excellent review of chip formation literature was conducted by Jawahir *et al.* From this review, a discussion on chip flow and curl (up, side, and back) is available to further understand chip geometry (Figure 2.8). Researchers determined there is a good correlation between friction angle and side-curl angle, with individual variations of .5-12 degrees. The chip side-curl also appears to be influenced by the straightness of the cutting edge, the perpendicularity of the cutting edge to the direction of cutting motion (a lack of perpendicularity creates variations in the chip-compression rate along its width), and the

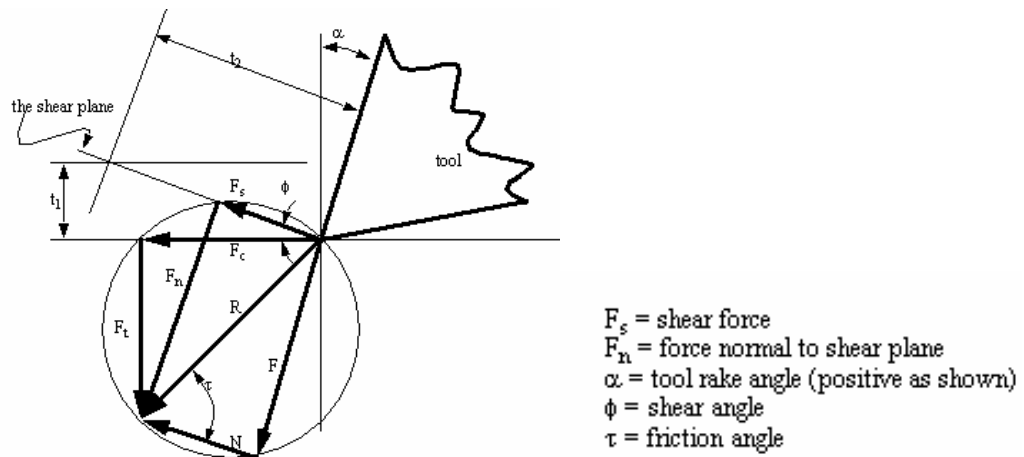


Figure 2.7: Merchant force circle [17].

presence of lubrication (which inhibits side curl by shortening the contact length). Chip back flow angle was observed to increase almost linearly with feed [25]. It is noted that the mechanics of chip flow and curl vary with the depth of cut. This paper suggests that there is still work to be done to determine the most influential factors affecting a chip's up-curl, side-curl, and back-flow [25]. Astakhov *et al.* [26] agrees, asserting that the chip flow direction and causes of curl are unclear, but that despite our lack of knowledge, chip curl can be initiated using a radiused groove on the tool rake face.

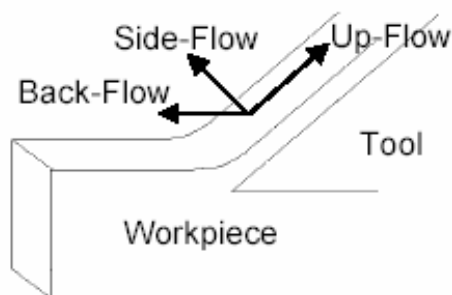


Figure 2.8: Chip flow diagram.

Chip curl is also a function of tool conductivity and friction along the tool-chip interface. Friction at the tool-chip interface is commonly accepted to be the shear stress of the workpiece material; and, increased temperatures soften the material. Following what is already known, it would seem increased temperatures lead to reduced friction and therefore smaller chip diameters. However, increased tool conductivity is known to raise the chip diameter [25]; this is due to the competing effect of increased material stiffness with reduced temperature. Which of the two factors is dominant? This is unknown, and probably varies with speed, material, temperature.

In addition to the side and up curls already discussed, Fang [27] introduced the idea of the lateral curl, which completes the story of how chips geometries are formed. The lateral curl explains a sort of twist that is seen in helical shaped chips. Seen in Figure 2.9, Fang is able to generate computerized images of chip geometries by inputting the up, side, and lateral curls.

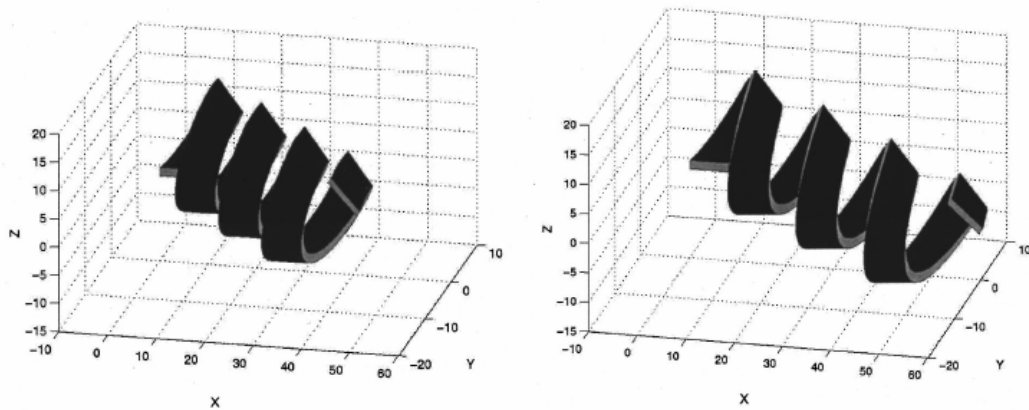


Figure 2.9: Computer generated chip geometries showing effect of lateral curl [27].

Observations indicate that the forces present on the chip will also affect its radius

of curvature away from the tool face, as shown in Figure 2.10. It has been observed that the radius of curvature decreases with rake angle and lubrication, creating curlier chips [23]. Note that a lower rake angle generally indicates increased friction [22]. Additionally, the cutting edge shape, and variations of material properties through the chip thickness (if the material's surface was previously strained by machining) may affect chip curl [22]. Thus, the work hardening characteristics of the work material are important. In 1978, Horne determined a method for predicting the chip radius (r) based on the shear angle (ϕ), rake angle (α), tool width (s), and depth of cut (d). Horne's equation is given here as (2.1).

$$r = \frac{d^2}{s \cos \alpha \sin \phi} \quad (2.1)$$

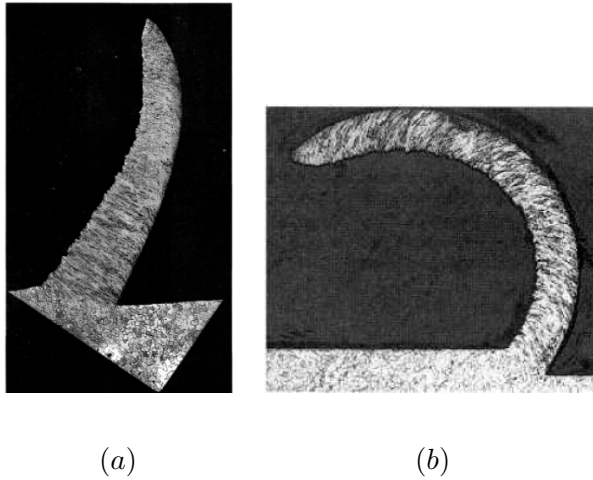


Figure 2.10: Chip curl in iron for (a) dry and (b) lubricated machining [22].

It was already stated that the cutting edge shape will affect chip flow, and lubrication is known to minimize the built up edge on the tool tip [23], which essentially alters the tool shape. Wang and Mathew showed a strong relationship between chip flow angle,

tool nose radius, and edge inclination [25]. Jacobson *et al.* [28] agreed that the formation of a built up edge (BUE) affects how the chips forms. A built up edge results in seizure and a stagnated layer. The stagnated layer grows until the material shears and cracks creating a new built up edge cutting face.

The discussion of chip curl up to this point has been solely concerned with the chip as it flows away from the tool face. However, observation of machining chips shows there is usually more than one radius present on the chip, with the largest being up to twice the size of the smallest. This larger radius occurs when the chip curls back to contact the workpiece surface, creating a bending moment [25]. This additional force on the chip will either cause fracture, or open up the radius of curvature during the chip's formation.

Interestingly, and obvious to all who have observed chips as they fly off a machine, Fang *et al.* [27] confirmed and explained previous assertions that chip formation problems have a non-unique solution, by discussing and refining Dewhurst's universal slip-line theory involving a plane-strain rigid-perfectly-plastic material. The non-uniqueness of this problem comes from the 4 equations (balance of forces in two directions; moment balance; tool-chip contact length), and 5 unknowns (4 slip-line field angles and the hydrostatic pressure where the workpiece outer surface meets the chip).

The discussion thus far has focused on milling or orthogonal cutting processes. In 2005, Ke looked at drilling chip formation [29]. He explained that the cutting speed variation along the cutting edge creates conical chips. The length of these conical and spiraling chips is directly related to the point and helix angle of the drill. Additionally, experiments showed that regardless of rake angle, spindle speed, or feed, the chip diameter

was the maximum to fit within the drill flute. As the depth of the drilled hole went deeper, Ke observed spiral chips becoming irregular and sheared.

Recently, work on chip formation has turned towards micro machining [30]. Jackson observed tight curled chips in the short regime of machining before the secondary shear zone develops. Because it is micro machining, this model includes the effect of tool bending; a new development in chip formation modeling. Additionally, Jackson's theory states that the primary chip curl is greatly affected by the presence of BUE, which agrees with earlier assertions that the tool tip shape/radius influences chip flow.

2.5 Chip Classification

Classifying chips is an important step to standardize discussions about what has been observed. In 1977, and again in 1993, ISO 3685 was issued, including a section on chips observed in turning operations; these same chip types are observed in milling and drilling and are shown in Figure 2.11.

Despite the standard provided by ISO, additional methods of classification have been developed by necessity. Kalpakjian [23] discusses chips based on the mechanics of formation: continuous chip with narrow, straight primary shear zone; chip with secondary shear zone at the chip-tool interface; continuous chip with large primary shear zone; continuous chip with built-up edge; segmented or nonhomogeneous chip; or discontinuous chip. Kalpakjian also classifies chips based on the following: continuous; built-up edge; serrated; and discontinuous (Figure 2.12). It seems researchers choose any combination of these when classifying their chips. For example, Davies [16] lists five types of chips: continuous














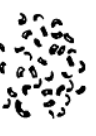
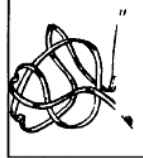



Table G.1 — Chip forms							
1 Ribbon chips ¹⁾	2 Tubular chips ¹⁾	3 Spiral chips	4 Washer-type helical chips ¹⁾	5 Conical helical chips ¹⁾	6 Arc chips ²⁾	7 Elemental chips	8 Needle chips
1.1 Long 	2.1 Long 	3.1 Flat 	4.1 Long 	5.1 Long 	6.1 Connected 		
1.2 Short 	2.2 Short 	3.2 Conical 	4.2 Short 	5.2 Short 	6.2 Loose 		
1.3 Snarled 	2.3 Snarled 		4.3 Snarled 	5.3 Snarled 			

Figure 2.11: ISO 3685 chip classification.

chips, chips with built up edge, shear localized chips (serrated), chips with periodic fracture (discontinuous), and segmental chips

Ning *et al.* [31] observed and named four chip types while ball nose end milling hardened steel: complete rolled chips, unstable chips, critical chips characterized by chatter, and severe chips characterized by too large a depth of cut. Interestingly, no adiabatic shear type chips were observed, which may be explained by the tool geometry or work material.

Viharos *et al.* [32] was interested in how to enable a machine to determine what types of chips it is creating. By choosing various classification schemes, he determined which parameters, measurable by the machine while cutting, best determined each chip type. These parameters included the cutting parameters along with aspects of the force and power inputs. His ability to predict chips using between 9 and 13 input parameters

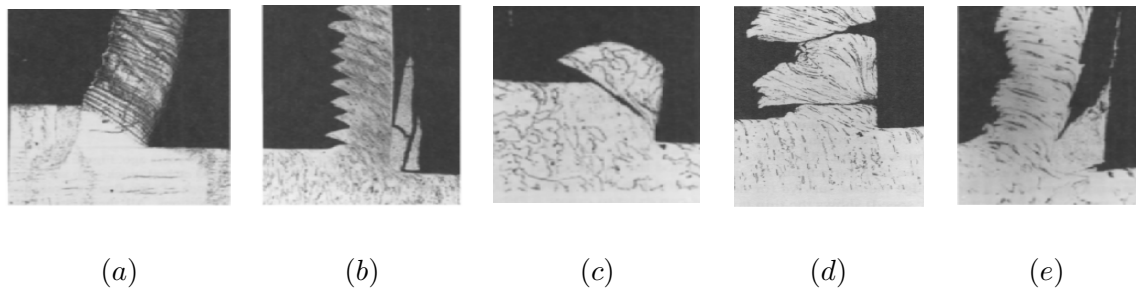


Figure 2.12: (a) continuous, (b) serrated with built up edge, (c,d) discontinuous, and (e) built-up edge [22].

was between 52% and 80%. From this, he hoped to create a system whereby the machine could adjust itself in real-time to create the desired type of chip.

2.6 Chip Breaking & Control

Extensive work on chip breaking has been pursued with the goal of easing problems from chip clogging or workpiece damage during the machining process. Methods to break the chip include variations of the tool geometry or even a piece of metal clamped to the face of the tool (chip-breaker) to interrupt the chip flow [23].

In addition to mechanically breaking the chip with a chip breaker or tool geometry variations, some researchers want to understand how to create discontinuous or broken chips that break due to shearing within the primary shear plane. Research on the milling of aluminum, with rake angles ranging from -5° to 35° , feeds ranging from 0.04 to 0.75 mm per rev, and speeds of 108,350 and 840 rev per min determined that by increasing the feed and decreasing the rake angle the type of chip produced will change from continuous to partially discontinuous, because a high feed combined with a large rake angle are required

to cut aluminum. Additionally, reducing the feed, speed, or rake angle while keeping the others high, can decrease the chip's continuity. Speed, feed, and rake angle were determined to be the main parameters affecting chip type [33].

Chip control charts are a standard method of observing and characterizing a material's chip formation behavior with the use of a certain tool (Figure 2.13). These may be used to determine the effectiveness of a certain chip breaker or other schemes to interrupt chip formation by illustrating how the chip size varies with feed rate and depth of cut. For a similar tool and material, a previous chip control chart may be used to determine the optimal feed and depth of cut required to optimize chip breaking. According to Zhou [34], "There is a chip-breaking condition: The chip will always break when the depth of cut is greater than the critical depth of cut and the feed rate is greater than the critical feed rate. Otherwise the chip will not break".

2.7 Finite Element Prediction

It is important to note that in addition to theory and experiment on chip formation, researchers use finite element analysis as a prediction tool, where the material is modeled as elastic-plastic [35]. This work verifies previous understanding of material and cutting models.

In Mamalis' work there was no comparison of chip shape with experiment, however a final comparison of cutting forces proved the model successful. Cutting forces affect the final chip shape; thus, this FEM is only a few steps away from predicting chip form.

Muraka *et al.* [36] determined from finite element investigation that increasing the

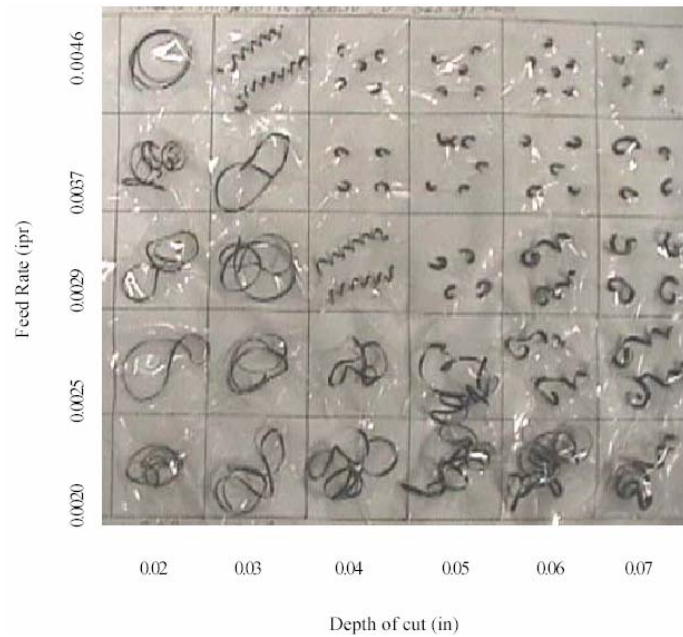


Figure 2.13: Sample chip breaking control chart: feed versus depth of cut [34].

cutting speed or feed will increase the rake and flank face temperature; in agreement with experimental results. Additionally, he found that when the rake angle is too high or too low the temperature increases.

And, Fukui *et al.* [37] successfully used finite element analysis to compare chip formation for high and low friction between the workpiece (AlCu2.5Si18) and tool (coated and uncoated cemented carbide tools). His analysis verified other researcher's observation that increasing the lubrication increases chip curl (Figure 2.14).

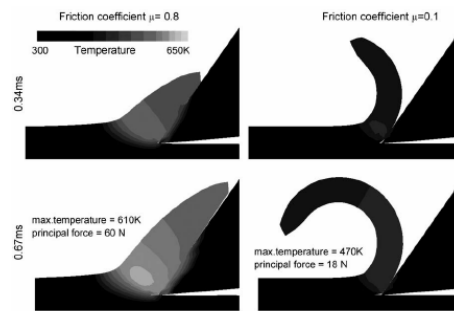


Figure 2.14: Simulation illustrating effect of lubrication on chip curl [37].

Chapter 3

Experimental Procedure

The previous efforts on controlling, classifying, and predicting chips are the first steps toward understanding chips to reduce their impact as a contaminant; however, previous research doesn't consider how the remaining chips will affect the function of the final part, assuming that once the machining operation is complete, any remaining chips can be easily removed.

As a first step to address this issue, it was desired to discover which of the following have the greatest impact on chip formation: feed, speed, lubrication, tool geometry or DOC. These parameters were chosen because they are easily varied in an established manufacturing configuration. From this information, trends of chip formation may be developed for use in industry to control chip geometries and sizes.

3.1 Chip Production and Collection

Both face milling and drilling were performed to mimic conditions within the Daimler Chrysler factory in Stuttgart, Germany. All chip types produced by each experiment were investigated, because they are all present under true machining conditions. Machining was conducted on a block of AlSi7Mg, the aluminum alloy used for Daimler-Chrysler's cylinder heads. The machining operations were conducted and planned by technicians and researchers from Daimler-Chrysler.

For milling, the controlled cutting parameters were speed, feed, lubrication (dry or wet), depth of cut (DOC), and tool geometry. For drilling, the controlled parameters were speed, feed, lubrication (minimum quantity lubrication or wet), and tool wear. The experiments were as shown in Tables 3.1 and 3.2. It should be noted from the tables of experiments that the milling experiments were unbalanced, affecting the possible method of analysis; this is discussed in sections 3.4 and 3.5.

The fully synthetic minimum quantity lubricant used was "Multicut Micro SP 51", which is made specifically for lubricant spraying. This MQL lubricant is 5 times the viscosity of the wet lubricant. The lubricant used for both "wet" conditions was "Ecocut HFN 10 LE", a low evaporative multipurpose chlorine-free lubricant and coolant.

Important angles for milling cutters are shown in Figure 3.1. Both milling cutters had a 125mm diameter and 6 PCD inserts as shown in Figure 3.2. Milling tool 1 had a radial rake of 4 degrees, lead angle of 0 degrees, and an axial rake angle of 0 degrees. Milling tool 2 is identical to milling tool 1 except for a lead angle of 15 degrees. The drilling tool was a single point 12mm diameter carbide twist drill with lubrication holes in the tip, a 120

Experiment	Feed (mm/tooth)	Speed (m/min)	Depth of Cut	Tool	Lubrication
1	0.1	1500	0.5	1	dry
2	0.1	3000	0.5	1	dry
3	0.2	1500	0.5	1	dry
4	0.2	3000	0.5	1	dry
5	0.2	3000	2.0	1	dry
6	0.1	1500	0.5	2	dry
7	0.1	3000	0.5	2	dry
8	0.2	1500	0.5	2	dry
9	0.2	3000	0.5	2	dry
10	0.2	3000	2.0	2	dry
11	0.1	1500	0.5	2	wet
12	0.1	3000	0.5	2	wet
13	0.2	1500	0.5	2	wet
14	0.2	3000	0.5	2	wet
15	0.2	3000	2.0	2	wet

Table 3.1: Milling experiments

Experiment	Feed (mm/tooth)	Speed (m/min)	Tool	Lubrication
16	0.15	188	new	MQL
17	0.15	377	new	MQL
18	0.30	188	new	MQL
19	0.30	377	new	MQL
20	0.15	188	new	wet
21	0.15	377	new	wet
22	0.30	188	new	wet
23	0.30	377	new	wet
24	0.15	188	worn	MQL
25	0.15	377	worn	MQL
26	0.30	188	worn	MQL
27	0.30	377	worn	MQL
28	0.15	188	worn	wet
29	0.15	377	worn	wet
30	0.30	188	worn	wet
31	0.30	377	worn	wet

Table 3.2: Drilling experiments.

degree point angle, a 55 degree chisel angle, and a 30 degree helix angle as seen in Figure 3.3. An image of the worn drilling tool edge is seen in Figure 3.4.

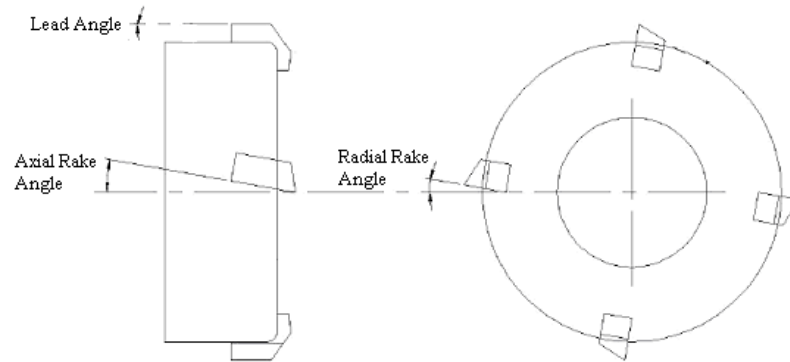


Figure 3.1: Important milling angles (modified from [8]).



Figure 3.2: Photographs of milling cutter 1.

These chips were collected in a bin placed below the machined surface, and carefully poured into plastic Ziploc bags for later analysis. See Figure 3.5.

3.2 Chip Classification - Separation of Chips by Type

It was first noticed that given a single set of cutting parameters (feed, speed, depth of cut, etc), up to five different chip sizes or geometries were produced. This is

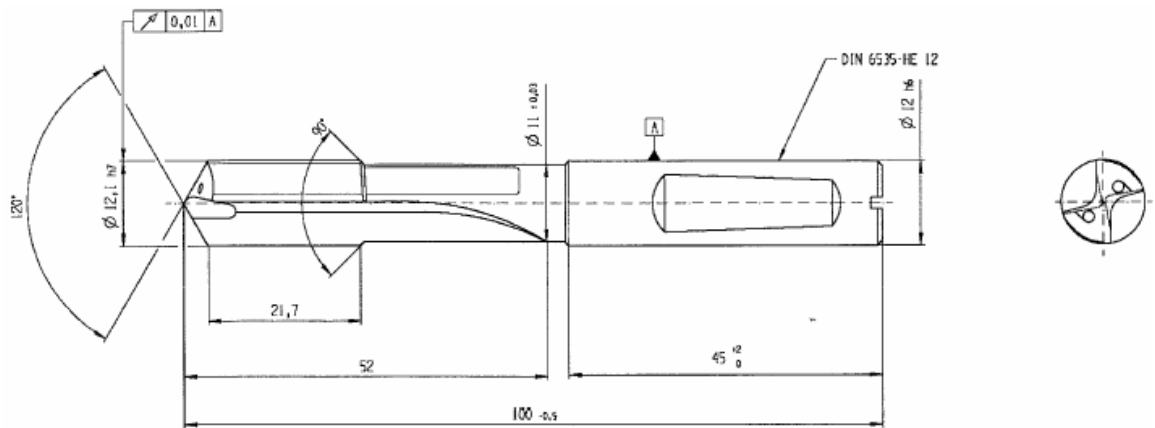


Figure 3.3: New drill specifications

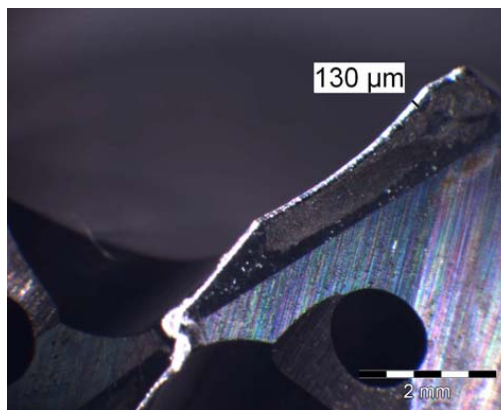


Figure 3.4: Photograph of the work drill cutting edge.



Figure 3.5: Experimental collection of machining chips.

understandable given the sensitive nature of the process. For example, slight variations in the machine vibrations or the material properties could produce variations in the chip. Additionally, newer models of chip formation, which use slip-line theory, propose that the final chip shape is nondeterministic [25].

To accurately represent the output of each experimental machining operation, the chips were divided into categories by size and shape (Figure 3.6). This involved very carefully untangling chips from each other to ensure their original form is preserved. A pattern quickly developed allowing the chips to be named based on a set number of classifications. These classifications are an extension of the ISO standard seen in Figure 2.11, and can be seen here in Figures 3.7 and 3.8.



Figure 3.6: Drilling and milling chips sorted by size and shape.

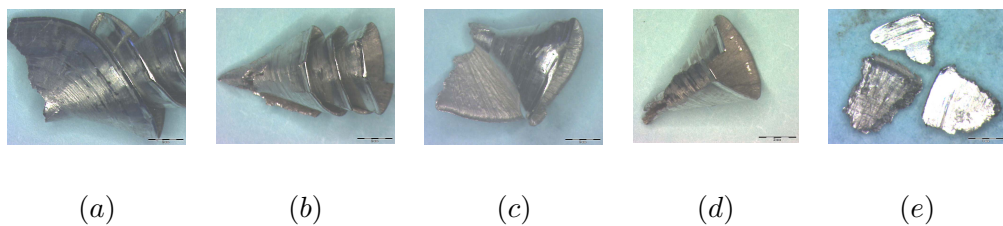


Figure 3.7: Drilling chip classification: (a) conical helical with wing, (b) conical helical, (c) cone with wing, (d) cone, and (e) flakes.

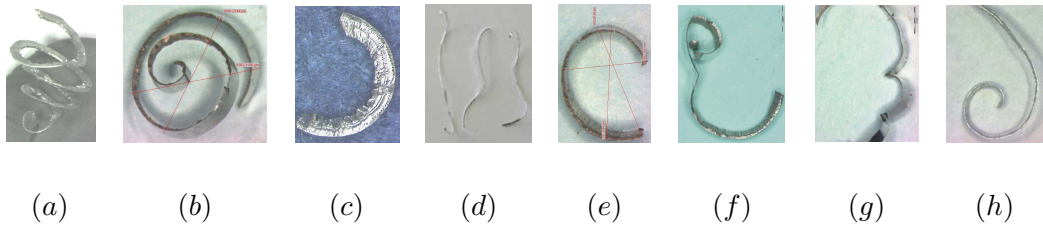


Figure 3.8: Milling chip classification: (a) washer spiral, (b) flat spiral or conical spiral, (c) washer, (d) ribbon, (e) oval, (f) spiral-arc, (g) arc, and (h) spiral-ribbon.

In addition to chip classification based on geometries, classification may be attempted by guessing at the dominant curl mechanism. This method is only interesting for the milling chips, because drilling chips are too constricted to vary significantly. The washer spiral and washer are characteristic of a dominant side curl. The flat spiral, conical spiral, spiral, and oval are characteristic of a dominant up curl. The ribbon and spiral-ribbon indicate a mostly straight flow. The arc and spiral-arc exhibit signs of combined lateral and up curl. This method can also be applied to the ISO standard as seen in Figure 3.9. Illustrations of up and side curl as they pertain to milling are seen in Figure 3.10.

3.3 Chip Measurement

Because the main goal of this research is to better understand how variations of cutting parameters affect the chip form so it can be controlled for optimum cleanability, it was imperative to measure any and all aspects of the chips that might affect their cleanability. Based on the assumptions presented in the introduction, the following aspects of the chips were measured (Figure 3.11): length, maximum and minimum diameter, maximum width, weight, wavelength (distance between each rotation of the chip), rotations, shear




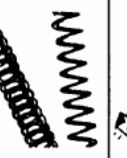

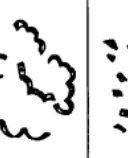







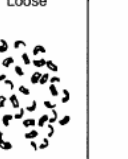


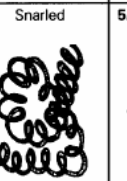

Straight		Up Curl		Side Curl		Up & Lateral Curl	
1 Ribbon chips ¹⁾	2 Tubular chips ¹⁾	3 Spiral chips	4 Washer-type helical chips ¹⁾	5 Conical helical chips ¹⁾	6 Arc chips ²⁾	7 Elemental chips	8 Needle chips
1.1 Long 	2.1 Long 	3.1 Flat 	4.1 Long 	5.1 Long 	6.1 Connected 		
1.2 Short 	2.2 Short 	3.2 Conical 	4.2 Short 	5.2 Short 	6.2 Loose 		
1.3 Snarled 	2.3 Snarled 		4.3 Snarled 	5.3 Snarled 			

Figure 3.9: ISO chip classification with dominant curl mechanism added.

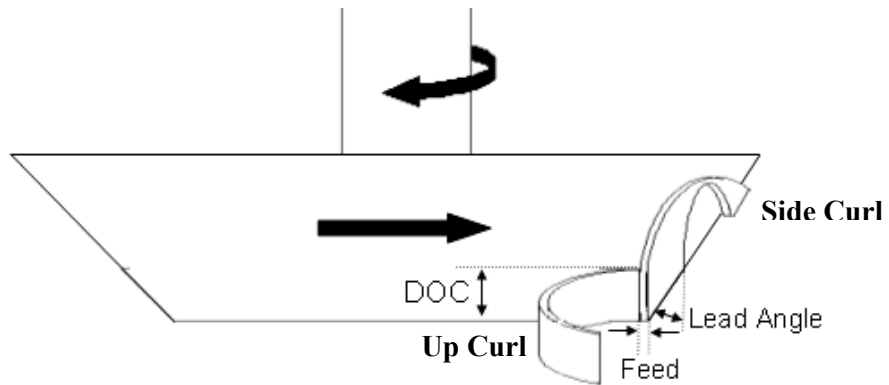


Figure 3.10: Up and side curl illustration for milling.

zone wavelength (distance between shear bands), and the shear zone height (distance between the peaks and valleys of the ridges produced by localized shear). For milling, because the mill cuts the chip along two surfaces (one in the direction of the depth of cut and one in the direction of the feed) the edge thickness was also measured. The shear zone wavelength, edge thickness, width, wavelength, and tooth height measurements were measured approximately 10 times for each chip and averaged. It's clear from Figure 3.11 d and e that this is necessary to average out the randomness and achieve an accurate representation of each chip

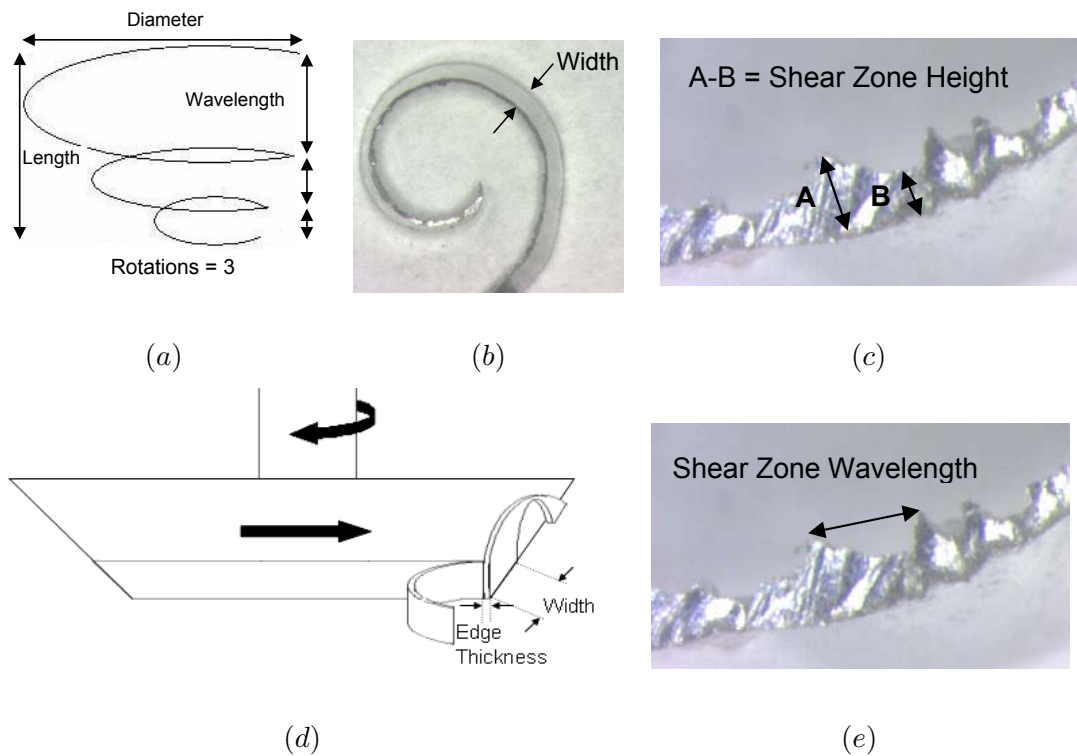


Figure 3.11: Chip geometry measurements: (a) rotations, wavelength, diameter, length (b) width (c) shear zone height (d) edge thickness and width (e) shear zone wavelength.

Measurements were taken using an Optical Coordinate Measuring Machine (OCMM),

consisting of a microscope and a camera that feeds output to a computer display. Distances are measured by clicking between two points on the computer screen, and are automatically calculated by the OCMM software depending on the image magnification. The precision of this machine was determined by measuring 1mm on a ruler 20 times; the standard deviation was 18.4 microns.

To properly orient each chip for these measurements, the dimension in question had to be placed in full view of the OCMM microscope. The chips were carefully placed in a piece of soft clay and rotated until the desired dimension was at its maximum; this is the true dimension, because as the chip rotated out of this plane in any direction, the dimension appeared smaller.

3.4 Design of Experiments

Using Taguchi's method of experimental design and analysis, it is possible to determine the dominant parameters affecting a particular measured output. A high and low value is selected for each of the controllable parameters of the experiment (such as speed and depth of cut). For each combination of the controllable parameters, the resultant chips geometries are measured (such as chip length and diameter).

As an example, consider an experiment where feed and speed are considered the controllable parameters and the chip weight is to be measured. If two values of feed and speed are chosen to represent high and low values, then 4 experiments are necessary to cover all possible combinations. For each experiment, a particular chip weight is measured. It is optimal to repeat the experiment multiple times to obtain the average output.

From the data, effect values are calculated, which indicate the relative influence of each controllable parameter. The effect of feed, for example, is calculated by subtracting the average of the measured weights when feed is low from the average of the measured weights when feed is high.

Additionally, it is possible to determine if there are important interactions between the controllable input values. For example, if feed and speed independently have no effect on the measured weight, then it's still possible that by varying feed and speed together a noticeable change in the weight may occur. To calculate interaction effects, the average of the weights when the feed or speed is low and the other is high is subtracted from the average of the weights when feed and speed are either both high or both low [38].

It was mentioned earlier that the milling experiments were unbalanced. This affects the milling analysis. For example, the high depth of cut experiments were only done for high feed and speed, therefore these results could not be included in the weight versus feed analysis because it would skew the high feed weight. Therefore, feed, speed, and lead angle calculations are based on experiments 1-4 and 6-9; lubrication calculations are based on experiments 6-9 and 11-14; and DOC calculations are based on experiments 4-5 and 14-15.

3.5 Correlation

The correlations (ρ) between varying the input parameters and the outputs were found mathematically, as shown in equation 3.1. A strong correlation between two parameters, in this case, requires there to be little second order interactions. X and Y are the inputs and outputs of the experiment (for example, X may be a vector of feeds and Y a

vector of chip weights); $Cov(X,Y)$ is the covariance or relationship of the data. The correlation value represents how close a linear regression is able to match the experimental data; a linear regression is appropriate because there are only two points: high and low. Due to the subjectivity of chip measurement, imperfect alignment with the optical measuring machine, and the inherent variability of chip formation (due to vibrations, material effects, temperature, etc.), a statistical correlation of greater than 80% (greater than 0.8 or less than -0.8) is assumed to be noteworthy. The milling analysis was conducted as discussed in the last section.

$$\rho(X, Y) = \frac{Cov(X, Y)}{\sigma(x)\sigma(y)} \quad (3.1)$$

3.6 Analysis of Variance using Matlab

For the drilling experiments, and some of the milling experiments, n-way analysis of variance was used in Matlab to determine the statistical relationship between the process variables and the measured parameters. Matlab describes n-way Anova as a method “to determine if the means in a set of data differ when grouped by multiple factors. If they do differ, you can determine which factors or combinations of factors are associated with the difference” [39].

Analysis of variance provides a statistical “p-value” between each controlled variable and measured variable. This value provides information on whether or not a “null hypothesis” (i.e. there is no variation in the measured output as the experiment’s variables are changed) is valid or not. If the p-value is close to zero, then the null hypothesis is

unlikely to be correct, and a relationship between the variables is concluded. P-values of less than 0.01 are considered significant in this analysis.

Chapter 4

Experimental Results and Analysis

As seen in Figure 3.6, for each individual experiment, there were multiple outputs. To rectify these into a single measured output for each input, the results were averaged based on the number of each type of chip. For example, if there were 8 chips of length A and 2 chips of length B, then the result of that experiment would be chips of length $[0.8(A) + 0.2(B)]$.

There was also the option to average the results based on the weight of each chip type. For example, if all the chips of length A were a combined weight of 3 grams, and all the chips of length B were a combined weight of 7 grams, then the final length would be $[0.3(A) + 0.7(B)]$. However, the data presented in this report was not averaged by weight, but by number as discussed above. This prevents one large chip from greatly skewing the data of many small chips.

Average values were used rather than the maximum or minimum measurement from each experiment because it was desired to see trends rather than focusing on outliers

that may be extremities caused by inconsistencies from nuances within each experiment.

The results given here are of correlation, effect, and p-values. The correlation suggests how well variations of the control variable match to variations of the measured chip parameters. The effect value quantifies, on average, how much of a change is expected in the measured output when the control variable is switched from low to high. A match between high correlation and high effect value indicates that a control parameter is significant. The p-value is used to confirm or cast doubt on this relationship. Additionally, a correlation may not be seen where a p-value indicates there is a relationship. Because the correlations require there to be no second order interactions, a p-value is useful in cases where multiple interactions are occurring simultaneously.

4.1 Milling

Tables 4.1, 4.2, and 4.3 contain the results of the correlations, effects, and p-values between each controlled input parameter and each measured output; calculated as discussed in sections 3.4, 3.5, and 3.6 respectively. A low value of lubrication is dry and a high value of lubrication is wet. Milling cutter 1 has a lead angle of 0 degrees (low) and Milling Cutter 2 has a lead angle of 15 degrees (high). The wavelength, edge thickness, and shear wavelength do not have experimental results for all the input variables, because they were only measured for experiments 1-4. This was done in the interest of time.

At the end of this section, table 4.4 provides photographs from the experiments to illustrate the trends discussed here.

	Weight	Rotations	Max Diam	Min Diam	Length	Wave-length	Width	Shear Zone Height	Shear Zone Height / Feed	Edge Thickness	Shear Wave-length
Speed	-0.13	-0.39	0.54	0.08	-0.55	0.41	-0.11	-0.34	-0.53	0.10	-0.79
Feed	0.24	-0.80	-0.42	0.50	-0.50	-0.52	0.26	0.85	0.30	0.98	0.33
Lubrication	-0.61	-0.58	-0.86	-0.18	-0.70		-0.55				
Lead Angle	0.58	0.37	0.11	-0.33	-0.24		0.95				
DOC	0.89	-0.65	0.46	0.39	0.92		1.00				

Table 4.1: Milling correlations. Significant values are boxed.

	Weight	Rotations	Max Diam	Min Diam	Length	Wave-length	Width	Shear Zone Height	Shear Zone Height / Feed	Edge Thickness	Shear Wave-length
Speed	-0.40	-0.40	4.28	0.17	-1.27	778.50	-37.42	-32.63	-0.14	8.15	-128.26
Feed	0.76	-0.82	-3.35	1.02	-1.15	-992.50	86.52	81.75	0.08	83.26	53.93
Lubrication	-2.50	-0.55	-3.06	-0.33	-0.95		-42.52				
Lead Angle	1.83	0.38	0.88	-0.66	-0.50		321.77				
DOC	15.58	-0.22	1.59	0.37	1.96		1558.29				
Speed-Feed	-1.24	0.15	-3.09	-0.43	-0.08	-1411.50	-22.10	-39.96	-0.22	-15.90	-81.96
Speed-Lub	-0.63	-0.15	-1.47	0.08	-0.42		-7.84				
Speed-LeadAngle	-0.30	0.16	-2.47	-0.91	1.06		21.55				
Feed-Lub	-0.09	0.44	0.58	-0.73	-0.12		-25.66				
Feed-LeadAngle	2.08	-0.10	3.46	1.24	0.75		-18.92				
Lub-DOC	-3.99	-0.01	0.52	0.85	0.09		37.05				

Table 4.2: Milling effects: average change in output value when going from low to high input value. Largest effects are boxed

	Weight	Rotations	Max Diam	Min Diam	Length	Width
Speed	0.08	0.008	0.6	0.02	0.31	0.33
Feed	0.04	0.007	0.4	0.007	0.57	0.19
Lubrication	0.04	0.006	0.09	0.03	0.22	0.19
Speed-Feed	0.13	0.04	0.65	0.07	0.44	0.25
Speed-Lub	0.17	0.02	0.19	0.13	0.43	0.66
Feed-Lub	0.7	0.007	0.42	0.01	0.78	0.3

Table 4.3: Milling p-values: significance of relationship between variables and measured parameters. Significant p-values are boxed.

The chip's weight is a function of its rotations, diameter, length, wavelength, width, and edge thickness; however these experiments indicate that the depth of cut has the strongest influence on the chip's weight. The depth of cut also influences the length and width of the chip. It is reasonable to assume the length and width will have a large influence on weight, because they establish two of the three largest dimensions of the chip.

The number of times a chip completes a rotation is determined by its length and wavelength, and is shown experimentally to be most influenced by the speed, feed, and lubrication. Feed also strongly positively correlates with edge thickness, and has strong effect values that say increasing feed will decrease the chip's wavelength and length. This is probably because the increased edge thickness causes the chip to be less ductile (dislocations cannot travel to the surface as easily), thus it breaks more easily. Additionally, the decreased wavelength (tighter spiral) with increased feed may cause the chip to make contact with the workpiece surface sooner and cause it to fracture.

The maximum diameter appears to be most influenced by lubrication, although the p-value in this case is not low enough to conclude there is a significant statistical relationship. According to Jawahir [25] this diameter of the chip occurs when the chip curls back and makes contact with the workpiece surface, creating a bending moment. This added force on the chip opens its diameter. The bending moment is about the point of the chip that is rigidly adhered to the workpiece, which is considered the shear zone by Jawahir. The presence of a coolant or lubricant will decrease the chip's ductility, which will inhibit the chip's ability to widen.

Of all the measured parameters of this experiment, the minimum chip diameter

has been most extensively studied by researchers; it occurs when the chip is first being cut, and is usually studied as up-curl but may be side-curl as well. According to previous researchers, the up-curl radius decreases for reduced rake angles (reduced cutting force), increased lubrication (reduced tool-chip contact) [23, 37], reduced tool width, and reduced depth of cut (reduced cutting force and chip stiffness) [40, 25]. Side curl is also affected by the tool's cutting edge perpendicularity and straightness [25]. Temperature increases, caused by speed or feed increases (except at very high speed when temperature goes down again), lead to reduced friction [36], and may also reduce the side curl and increase the up curl.

So how does all this compare with the experimental results for minimum chip diameter given above? It's interesting because the feed shows the only statistically significant relationship with minimum chip diameter. So then, what about previous observations on the influence of rake angle, lubrication, depth of cut, and temperature? It is possible that these effects are indications of other things. Decreasing the rake angle will decrease cutting forces and friction. Decreasing the depth of cut also decreases the cutting forces. Decreasing temperature increases friction and may increase the chances for built up edge. It is forces that determine chip flow, and in this experiment, increased feed resulted in an increased cutting force, resulting in a larger diameter chip. It is also important to note that when previous researchers mention an increase in depth of cut, they are discussing the orthogonal cutting model; for milling, the depth of cut may be seen as the feed. Therefore, the results do not disagree.

Length appears to be most influenced by the depth of cut, although the p-value is

not statistically significant. Traditionally, length is shown on chip breaking charts, which indicate that an increase in the depth of cut and/or feed will achieve broken chips [34]. The apparent discrepancy between the observations from these experiments and those of previous chip breaking charts is in how the chips are measured. On the chip breaking chart, the chip seems to go from a large diameter short chip to a small diameter long chip, and then to a small broken chip. The length is measured perpendicular to the maximum chip diameter, which in this case increases with the depth of cut. This effect is seen in table 4.4. Additionally, increasing feed does appear to decrease the chip's length, but the correlation and effect is inconclusive. Researchers indicate that the feed, speed, and rake angle may be important for triggering a transition to discontinuous chips [33]; however these chips showed no signs of discontinuity.

Results for the chip's wavelength are inconclusive. It's possible that something other than feed or speed will show a greater correlation, however data was not taken to show this. The wavelength is a function of the chip's curl and length, which would indicate that the feed, speed and depth of cut are most likely the influential parameters. Additionally, increased backflow with respect to the side or up flow will increase the wavelength, and back flow has been observed to increase with feed [25].

The chip's width should theoretically be the depth of cut divided by the cosine of the lead angle (as it was defined in section "chip classification"); and, the experimental results show the lead angle and the depth of cut to be almost 100% correlated to the chip's width. However, the experimental values show the chip's width to be almost 20% greater than predicted. It is likely that the chip expands along the tool in the direction of cut

as it tries to relieve the compressive force it feels from the cutting tool (Poisson swelling). Strangely, although the correlation values are extremely high for this relationship, the p-values show no relationship. This will require additional investigation.

The shear zone height is caused by shear in the primary shear plane, and Flom [11] observed that increasing the speed will increase the degree of adiabatic shear; this is due to temperature swells weakening the material. Interestingly, the experimental results shown here indicate that it is feed, not speed, that most influences the shear zone height. This is due to the shear zone height being some fraction of the edge width. It may be that the more appropriate way of looking at the degree of shear is as the shear zone height divided by the feed (the dimensionless or relative shear zone height); because as this increases, the chip is considered more "sheared", which is what Flom was observing. The experimental results for shear height divided by feed indicate that speed has a stronger influence; but it is inconclusive. The effect values indicate that a combination of feed and speed is most influential on the degree of shear.

Speed has a noticeable correlation with and effect on the shear zone wavelength. This agrees exactly with Davies' [16] observations on the influence of speed on shear zone wavelength. This also corroborates Flom's observations of increased adiabatic shear with increasing speed. As the wavelength decreases, the degree of adiabatic shear is more severe.

The edge thickness is theoretically directly related to the feed, and the experimental results agree that feed is the most important parameter. The edge thickness tended to be slightly less than the feed, due to the mechanics of milling chip formation (i.e. the tool's thickness of cut is variable with its maximum value the feed). Kalpakjian [23] also

says the edge thickness may be increased by lowering the rake angle, increasing friction, or lowering the shear angle. Kishawy [24] asserts that edge thickness will be increased by tool wear and cutting speed. Unfortunately, the observations of these researchers are not verified or disproved by this experiment because the edge thickness was not measured over all the experiments; it was only observed over changing feeds and speeds.

In addition to the correlation and effect values presented above, observations of the chip geometries indicate a correlation between the lead angle of the tool and the chip flow. This was determined from classifying the chips based on dominant direction of curl (experimental procedure). Chips produced by milling tool 1 (0 degree lead angle) were more likely to show signs of side curl than chips produced by milling tool 2 (15 degree lead angle), which were mostly characterized by up curl. This is because the side curl is affected by the tool's cutting edge perpendicularity and straightness [25]. Both showed signs of lateral curl.

4.2 Drilling

Tables 4.5, 4.6, and 4.7 contain the correlation, effect, and p-values between the the measured parameters of the drilling chips and the controlled variables. As with milling, a low value of lubrication is MQL, whereas a high value is wet. For wear, a low value is a new tool, and a high value is a worn tool. The Shear Zone Height, Wavelength, and Shear Zone Wavelength were not measured for the worn tool.

At the end of this section, table 4.8 provides photographs from the experiments to illustrate the trends discussed here.

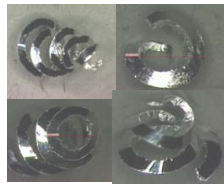


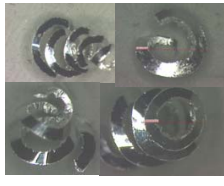

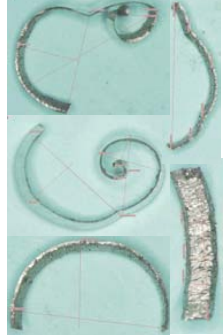


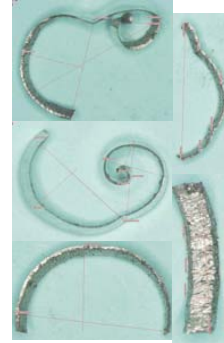

Variable	Experiment	Low	High
speed	dry, high feed, low DOC, tool 1		
feed	dry, low speed, low DOC, tool 1		
lubrication	tool 1, low DOC, high speed, high feed		
lead angle	low DOC, dry, high speed, low feed		
depth of cut			

Table 4.4: Photos of typical milling experimental outputs.

	Weight	Rotations	Max Diam	Length	Wavelength	Width	Shear Zone Height	Shear Height/Feed	Shear Wavelength
Speed	0.16	0.2	-0.09	0.19	-0.44	-0.16	-0.22	-0.18	-0.21
Feed	-0.24	-0.51	0.02	-0.53	0.71	0.04	0.75	0.44	0.44
Lubrication	-0.71	-0.51	-0.67	-0.39	0.33	-0.29	0.12	0.11	-0.55
Wear	-0.44	-0.28	0.20	-0.55		-0.28			

Table 4.5: Drilling correlations.

	Weight	Rotations	Max Diam	Length	Wavelength	Width	Shear Zone Height	Shear Height/Feed	Shear Wavelength
Speed	10.39	0.63	-0.27	0.71	-940.50	-138.75	-26.75	-0.06	-71.00
Feed	-15.14	-1.13	0.07	-2.01	1529.50	34.5	92.75	0.14	150.50
Lubrication	-45.26	-1.13	-2.01	-1.46	712.00	-241.25	14.75	0.035	-190.00
Wear	-28.39	-0.63	0.60	-2.06		-231.25			
Speed-Feed	-9.01	-0.38	-0.83	-0.30	32.00	-365.5	-45.25	-0.18	-178.00
Speed-MQL	-3.79	-0.38	-0.17	-0.18	5.50	-138.75	-44.25	-0.17	43.50
Speed-Wear	-9.01	-0.38	-0.49	-1.01		-368.75			
Feed-MQL	9.84	0.88	-0.73	0.80	-143.50	-190.5	23.25	0.09	-53.00
Feed-Wear	10.66	0.38	0.37	0.18		16			
Lub-Wear	14.69	0.38	-0.53	0.72		-41.75			

Table 4.6: Drilling effects: average change in output value when going from low to high input value. Largest effects are boxed.

	Weight	Rotations	Max Diam	Length	Width
Speed	0.22	0.004	0.73	0.16	0.55
Feed	0.10	0.0003	0.92	0.006	0.88
Lubrication	0.002	0.0003	0.04	0.02	0.32
Wear	0.01	0.004	0.44	0.005	0.34
Speed-Feed	0.28	0.03	0.30	0.52	0.15
Speed-MQL	0.64	0.03	0.83	0.69	0.55
Speed-Wear	0.28	0.03	0.53	0.07	0.15
Feed-MQL	0.25	0.0009	0.35	0.12	0.42
Feed-Wear	0.21	0.03	0.62	0.69	0.94
Lub-Wear	0.11	0.03	0.49	0.16	0.86

Table 4.7: Drilling P-Values: a value below 0.01 indicates the relationship is significant.

According to these results, lubrication plays the greatest role in determining chip weight. This may be explained by the mechanism of lubrication. The cutting oil comes directly out of the tool, and is most likely breaking the chips as it blasts out. Additionally, observations of the chips showed that those cut with lubrication tended to be far more brittle than those cut with MQL. This may be a result of thermal shock to the chip as it is forming.

Based on the effect values, Lubrication appears to play a role in determining the chip's maximum diameter, however the correlation and p-values show no statistical significance for this relationship. Ke observed that regardless of rake angle, spindle speed, or feed, the chip diameter was solely a function of the drill flute diameter [29]. Because only one drill was used for these experiments, Ke's observations cannot be verified.

Feed and tool wear are shown to play a role in determining the chip's length. Interestingly, length is not affected by lubrication, which would have made sense due to the brittle nature of chips cut with lubrication. Length was shown by Ke [29] to be determined by the depth of the hole (as the depth of the drilled hole increases, spiral chips become irregular and sheared) and the point and helix angle of the drill, which in this case could be indicated by tool wear.

There are no significant relationships seen for the rotations, width, or shear wavelength. The width was shown by Ke [29] to be most affected by the length of the tool's cutting edge (because it is confined to this). Based on the observations of Davies et al. [16] the shear zone wavelength should correlate to the speed; however, it's likely that because of the high variation of speed along the chip width during cutting, the shear zone does not

follow the same pattern as milling or turning.

The shear zone height during drilling matches the results for milling, where the dominant factor is feed. The shear zone height may be considered a fraction of the total chip thickness, where nothing else is causing a transition in shear.

The wavelength appears to have some correlation with the cutting feed. The chip is thicker and therefore stiffer as the feed increases, which would reduce its tendency to be deformed by friction into a small wavelength while attempting to flow up and around the drill flute.

4.3 Chip and Burr Control

Burr formation during milling is most determined by the depth of cut, the exit angle, and the exit order sequence (axial and radial rake angles). Depth of cut is known to increase chip weight and burr size. Because this research on chip formation did not discuss the effects of the axial and radial rake angles, it is unclear if the optimization of burr formation will match optimization of chip formation with respect to these parameters. For burr formation, it is possible to eliminate the effect of the depth of cut by creating secondary rather than primary burrs. This is accomplished by choosing the correct exit angle and exit order sequence for the material. For chip formation, reducing the chip weight with depth of cut requires finding the transition point on the chip breaking control chart.

Burr formation during drilling is determined by the thrust force (feed) and the exit angle (based on part geometry and orientation). The exit angle has no effect on chip formation, thus it is best to choose this to minimize burr formation. Feed is known to

Variable	Experiment	Low	High
speed	MQL, new tool, low feed		
feed	MQL, worn tool, low speed		
lubrication	new tool, high feed, low speed		
tool wear	high speed, low feed, oil lubrication		

Table 4.8: Photos of drilling experimental results.

increase chip wavelength, which for milling is a good thing to reduce the chances of chip entanglement; however, for drilling chips, a small wavelength means there is no room for entanglement; it is only when the wavelength increases that entanglement becomes possible. Thus, lower feed may be best in all cases.

Remember, the decisions on what chip types will be more or less cleanable are only guesses, and until concrete research is done to determine the most desirable chip, it is still uncertain how to best combine knowledge on burr and chip formation for optimal process parameters.

Chapter 5

Conclusions

Based on the assumptions of this paper, where the optimal chip is likely short, lightweight, with a large wavelength, and few rotations. The optimal milling chip is produced with increased speed, increased lubrication, decreased feed, and decreased depth of cut. For drilling, the optimal chip is accomplished through increased lubrication, decreased speed, and increased feed. It is observed through the influence of tool wear that additional research on the influence of tool geometry should be studied to understand its effects on chip geometry.

5.1 Summary

- Milling
 - Increased depth of Cut increases the chip's weight, length, and width; until chip breaking occurs.
 - Higher lead angles increase the chip's width and consequently its stiffness.

- The presence of a lubricant decreases rotations, and decreases the chip’s maximum diameter.
 - Increased feed reduces the number of rotations, decreases wavelength, increases the minimum diameter, and increases the shear zone height and edge thickness.
 - Increased speed decreases the number of rotations and the distance between the shear peaks.
- Drilling
 - Increased speed increases the chip’s rotations
 - Tool wear influences the rotations and length, indicating that tool geometry should be further investigated.
 - Lubrication reduces the rotations, maximum diameter, and weight of the chips.
 - Increased feed reduces rotations and chip length, and increases the chip’s wavelength and shear zone height.

5.2 Future Work

This research is just the start to understanding how process parameters affect the final chip geometry. With these in place it is possible to conduct further experiments, which may focus on the process parameters deemed most influential. Additionally, much research is required to establish what aspects of the chip determine if it will be a problem for the component cleanliness or not. A methodical investigation of chip cleanability must be pursued to determine the effectiveness of current cleaning techniques (such as water jets

and ultrasound) for removing the observed chip morphologies. This may include research on drag, adhesion, and various methods of cleaning. Then by combining chip prediction with this knowledge, part cleanability can be maximized. Additionally, understanding why and how certain chip types become a contamination issue can be incorporated into design for cleanability at level I.

Bibliography

- [1] K. Berger. Burrs, chips and cleanness of parts - activities and aims in the german automotive industry, 2006.
- [2] J.M. Sipitkowski. Design for cleanability: Part geometry and surface finish. *Precision Cleaning*, 1(1), 1993.
- [3] J.M. Sipitkowski. Design for cleanability: Part material selection. *Precision Cleaning*, 2(1), 2004.
- [4] L. Gillespie. *Deburring and edge finishing handbook*. Society of Manufacturing Engineers, second edition, 1999.
- [5] M. Avila, J. Gardner, C. Reich-Weiser, S. Tripathi, A. Vijayaraghavan, and D. Dornfeld. Strategies for burr minimization and cleanability in the aerospace and automotive industry. 2006.
- [6] D.A. Dornfeld. Strategies for preventing and minimizing burr formation. *Proc. Intl Conf. On High Performance Cutting*, pages 83–99, 2004.

- [7] K. Berger. An overview of the status and trends for burr activities in the automotive industry. *7th Int'l Conf. on Deburring and Surface Finishing*, 2004.
- [8] S. Tripathi and D. Dornfeld. Review of geometric solutions for milling burr prediction and minimization. *Proceedings of the Institution of Mechanical Engineers, Part B, Journal of Engineering Manufacture*, 2005.
- [9] A.E. Bayoumi and J.Q. Xie. Some metallurgical aspects of chip formation in cutting ti-6wt. *Materials Science and Engineering A: Structural Materials: Properties, Microstructure and processing*, 190(1-2):173–180, 1995.
- [10] W. Shefelbine and D. Dornfeld. Influences on burr size during face-milling of aluminum alloys and cast iron. *LMA Reports*, 2004.
- [11] D.G. Flom, R. Komanduri, and M. Lee. High-speed machining of metals. *Annual Review of Materials Science*, 14:231–278, 1984.
- [12] P.K. Wright and E.M. Trent. *Metal Cutting*. Butterworth-Heinemann, 2000.
- [13] T. Ozel and T. Altan. Determination of workpiece flow stress and friction at the chip-tool contact for high-speed cutting. *International Journal of Machine Tools and Manufacture*, 40(1):133–152, January 2000.
- [14] M. Davies, T. Burns, and T. Schmitz. High-speed machining processes: dynamics on multiple scales. *Proceedings of the Dynamics and Control of Mechanical Processing*, 2000.
- [15] Y. Sang, M. Dube, and M. Grant. Atomic friction. 2001.

- [16] M. Davies and T. Burns. Thermomechanical oscillations in material flow during high-speed machining. *Philosophical Transactions of the Royal Society A: Mathematical, Physical and Engineering Sciences*, 359(1781):821–846, 2001.
- [17] H. Jack. Merchant’s force circle with drafting, 2001.
- [18] F. Klocke. Basics of high performance cutting and mechanical and thermal characteristics. *Aachen Conference*, 2005.
- [19] M.C. Shaw. *Metal Cutting Principles*. Oxford University Press, 2005.
- [20] G. Warnecke and S. Siems. Dynamics in high speed machining, 1993.
- [21] H. Schulz. Influence of heat treatment and cutting parameters on chip formation and cutting forces. *Proceedings of the Third International Conference on Metal Cutting and High Speed Machining*, pages 69–78, 2001.
- [22] T.H.C. Childs, K. Maekawa, T. Obikawa, and Y. Yamane. Metal machining - theory and applications. *Elsevier*, 2000.
- [23] S. Kalpakjian. *Manufacturing processes for engineering materials*. addison wesley, third edition, 1997.
- [24] H.A. Kishawy, M. Dumitrescu, E.-G. Ng, and M.A. Elbestawi. Effect of coolant strategy on tool performance, chip morphology and surface quality during high-speed machining of a356 aluminum alloy. *International Journal of Machine Tools & Manufacture*, 45:219–227, 2005.

- [25] I.S. Jawahir and C.A. Van Luttervelt. Recent developments in chip control research and applications. *42(2):659–693*, 1993.
- [26] V.P. Astakhov, S.V Shvets, and M.O.M. Osman. chip structure classification based on the mechanics of its formation. 1996.
- [27] N. Fang, I.S. Jawahir, and P.L.B. Oxley. A universal slip-line model with non-unique solutions for machining with curled chip formation and a restricted contact tool. *International Journal of Mechanical Sciences*, 43:580–557, 2001.
- [28] S. Jacobson and P. Wallen. A new classification system for dead zones in metal cutting. *International Journal of Machine Tools & Manufacture*, 28(4):529–538, 1988.
- [29] F. Ke, J. Ni, and D.A. Stephenson. Continuous chip formation in drilling. *International Journal of Machine Tools & Manufacture*, 45:1652–1658, 2005.
- [30] M.J. Jackson. Primary chip formation during the micromachining of engineering materials. *Proc. IMechE Part B: J. Engineering Manufacture*, 219:245–254, 2005.
- [31] Y. Ning, M. Rahman, and Y.S. Wong. Investigation of chip formation in high speed end milling. *Journal of Materials Processing Technology*, 113:360–367, 2001.
- [32] Z.J. Viharos, S. Markos, and C. Szekeres. Ann-based chip-form classification in turning. *XVII IMEKO World Congress Metrology in the 3rd Millennium*, pages 1469–1473, 2003.
- [33] A.S. Shouckry. Zones and boundaries between different types of chip. 69:345–353, 1981.

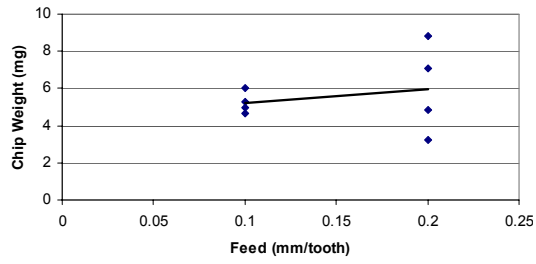
- [34] L. Zhou. *Machining Chip-Breaking Prediction with Grooved Inserts in Steel Turning*. PhD thesis, Worcester Polytechnic Institute, 2001.
- [35] A.G. Mamalis, M. Horvath, A.S. Branis, and D.E. Manolakos. Finite element simulation of chip formation in orthogonal metal cutting. *Journal of Materials Processing Technology*, 110:19–27, 2001.
- [36] P.D. Muraka, G. Barrow, and S. Hinduja. Influence of the process variable on the temperature distribution in orthogonal machining using the finite element method. *International Journal of Mech. Sci.*, 21:445–456, 1979.
- [37] H. Fukui, O. Junya, O. Naoya, M. Hideki, and T. Keiichi. Cutting performance of dlc coated tools in dry machining aluminum alloys. *Surface and Coatings Technology*, 187(1):70–76, 2004.
- [38] Ealey. *Quality by Design, Taguchi Methods and US Industry*. Irwin Professional Publishing, second edition, 1984.
- [39] MATLAB, June 2002. Version 6.5.0.180913a Release 13.
- [40] J.G. Horne. A new model for initial chip curl in continuous cutting. *Int. J. Mech. Sci.*, 20:739–745, 1978.

Appendix A

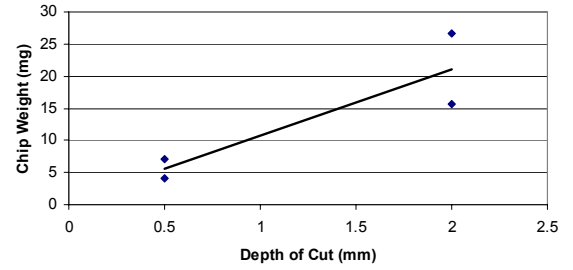
Graphs of Milling Correlations & Effects

The correlation and effect values for each measured parameter could not be calculated over the entire range of experiments, because there was not a balance of experiments. For example, the high depth of cut experiments were only done for high feed and speed, therefore these results could not be included in the weight versus feed analysis because it would skew the high feed weight. Therefore, feed, speed, and lead angle calculations are based on experiments 1-4 and 6-9; lubrication calculations are based on experiments 6-9 and 11-14; and DOC calculations are based on experiments 4-5 and 14-15.

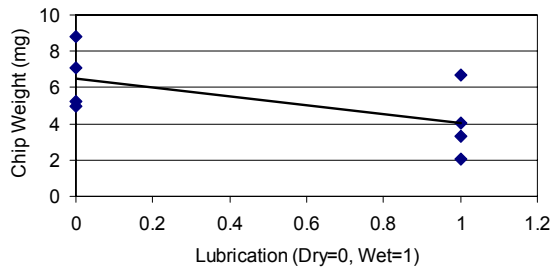
Each diamond on a graph represents the numerical (rather than weight) averaged output of all the chips from one experiment.



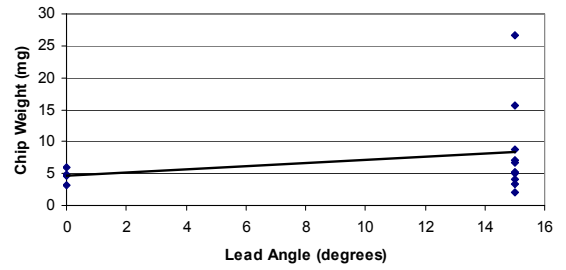
(a)



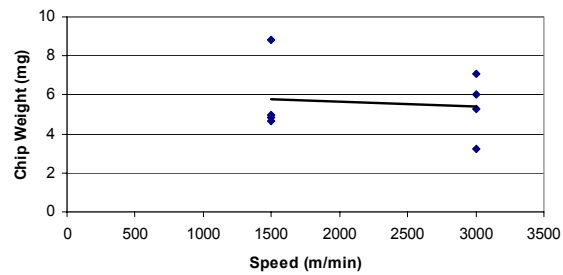
(b)



(c)



(d)



(e)

Figure A.1: Effect of process parameters on chip weight for milling: (a) feed (b) depth of cut (c) lubrication (d) lead angle (e) speed.

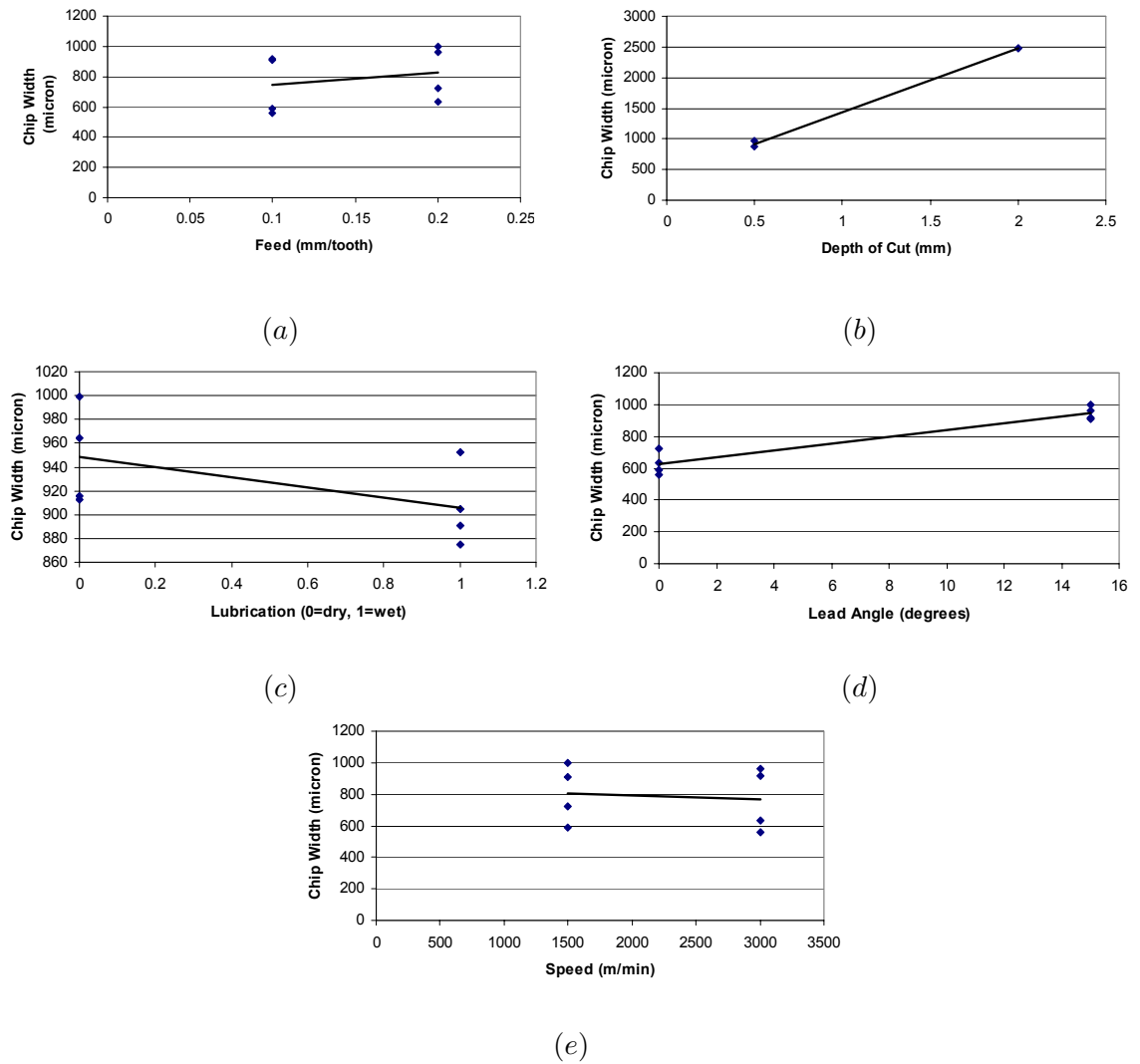
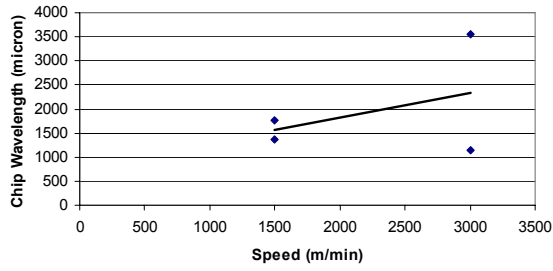
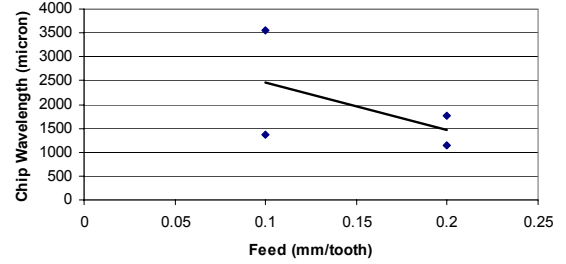


Figure A.2: Effect of process parameters on chip width for milling: (a) feed (b) depth of cut (c) lubrication (d) lead angle (e) speed.

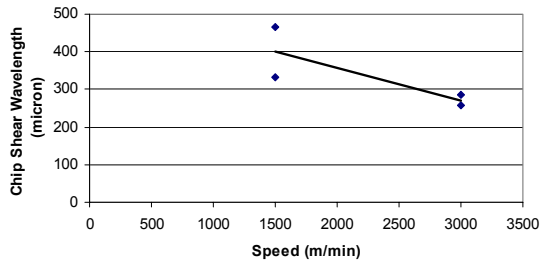


(a)

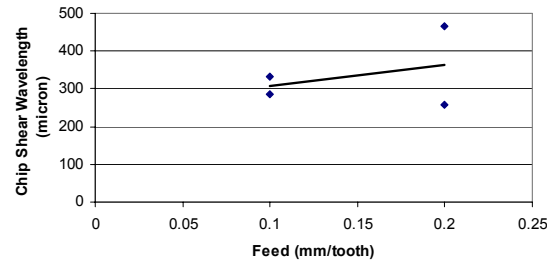


(b)

Figure A.3: Effect of process parameters on chip wavelength for milling: (a) speed (b) feed.

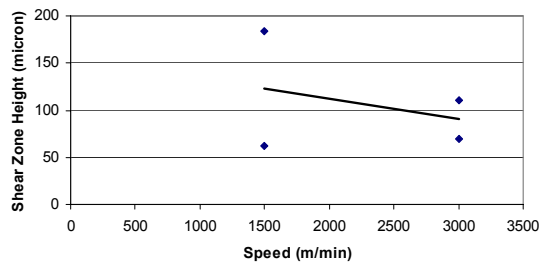


(a)

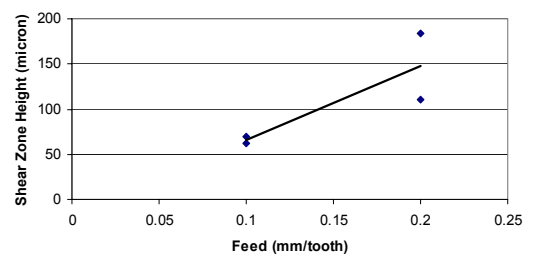


(b)

Figure A.4: Effect of process parameters on chip shear zone wavelength for milling: (a) speed (b) feed.

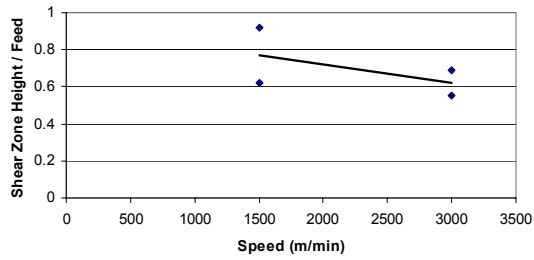


(a)

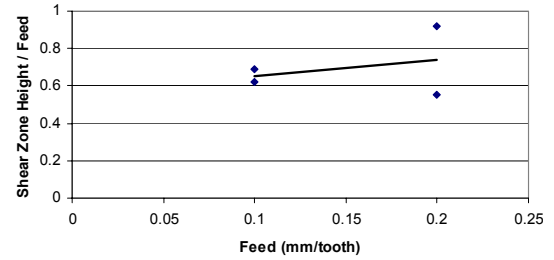


(b)

Figure A.5: Effect of process parameters on chip shear zone height for milling: (a) speed (b) feed.

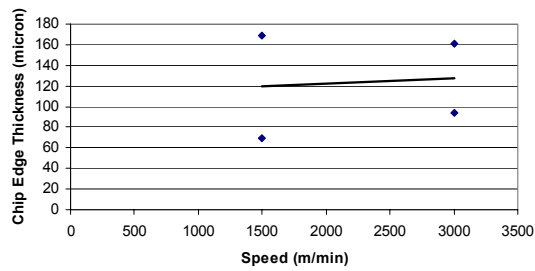


(a)

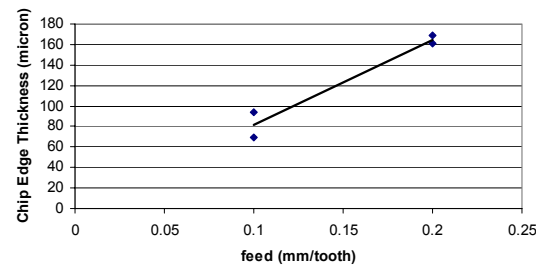


(b)

Figure A.6: Effect of process parameters on chip shear zone height divided by the feed for milling: (a) speed (b) feed.

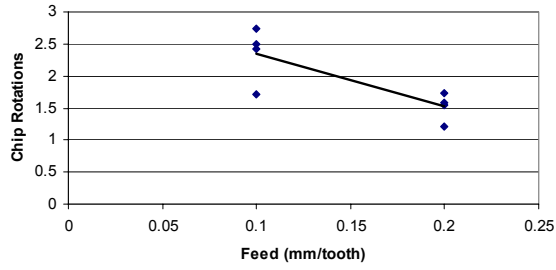


(a)

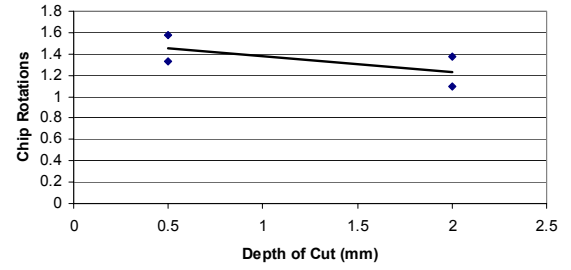


(b)

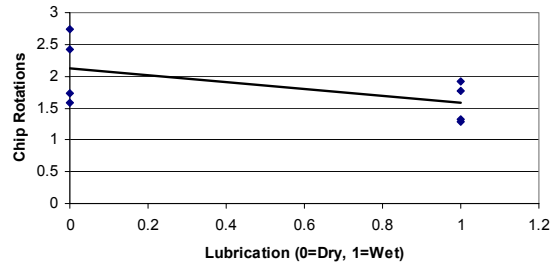
Figure A.7: Effect of process parameters on chip edge thickness divided by the feed for milling: (a) speed (b) feed.



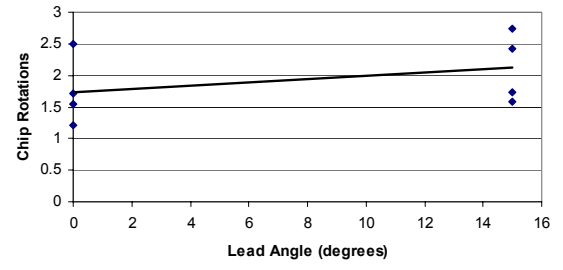
(a)



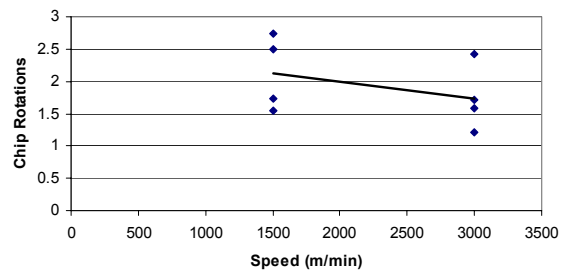
(b)



(c)

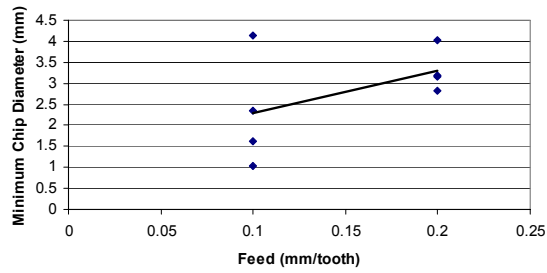


(d)

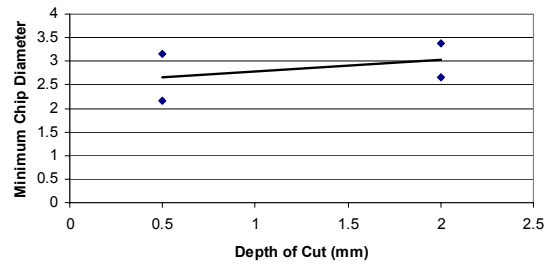


(e)

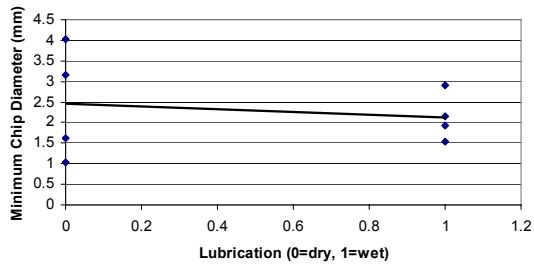
Figure A.8: Effect of process parameters on chip rotations for milling: (a) feed (b) depth of cut (c) lubrication (d) lead angle (e) speed.



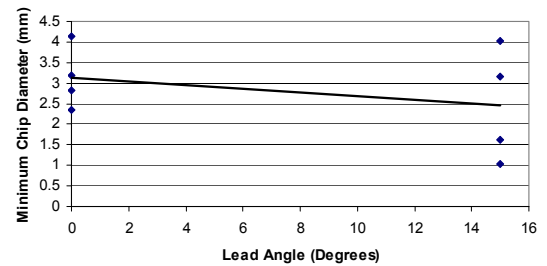
(a)



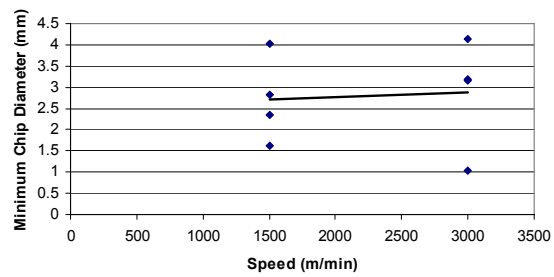
(b)



(c)



(d)



(e)

Figure A.9: Effect of process parameters on the chip minimum diameter for milling: (a) feed (b) depth of cut (c) lubrication (d) lead angle (e) speed.

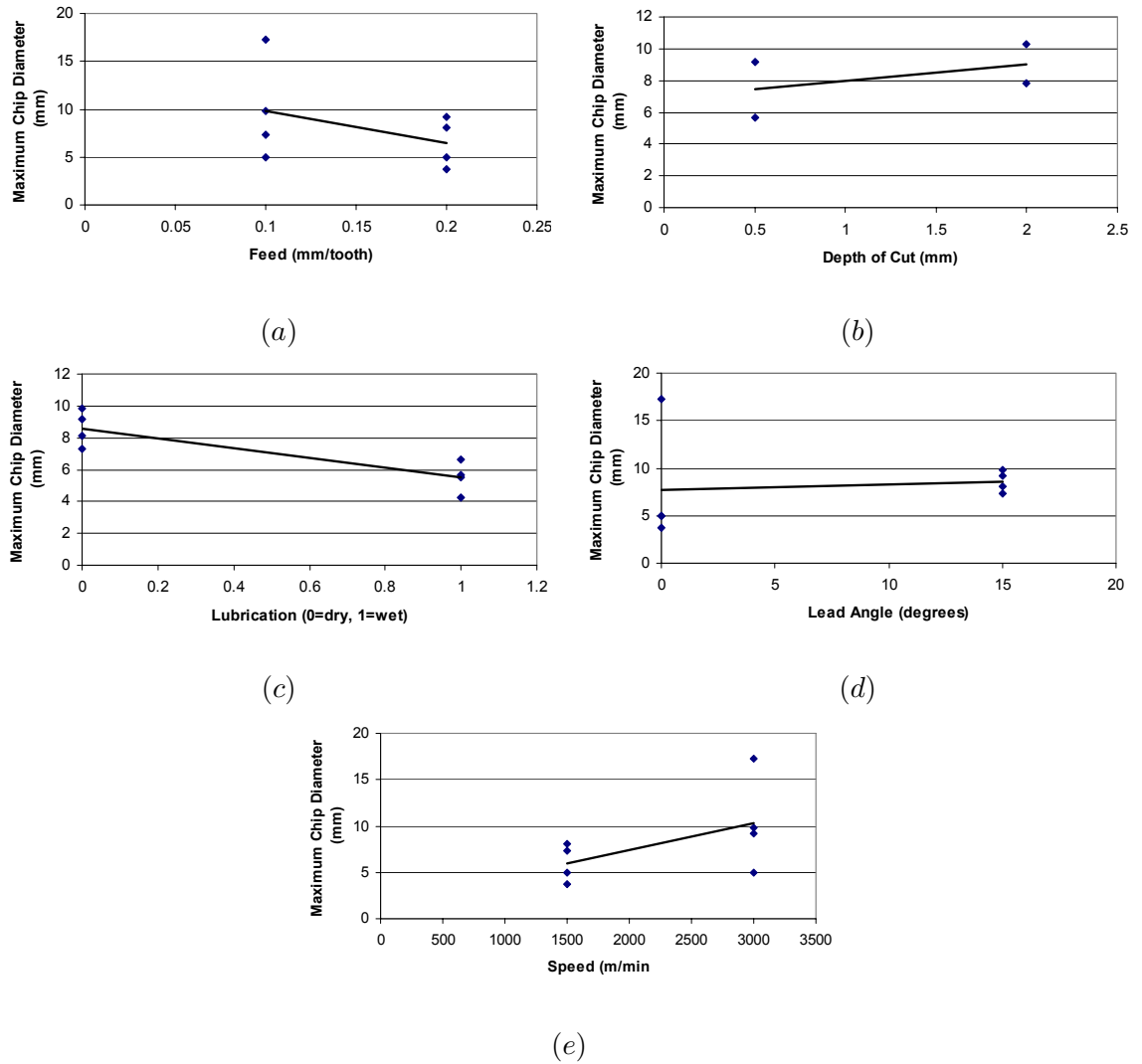


Figure A.10: Effect of process parameters on the chip maximum diameter for milling: (a) feed (b) depth of cut (c) lubrication (d) lead angle (e) speed.

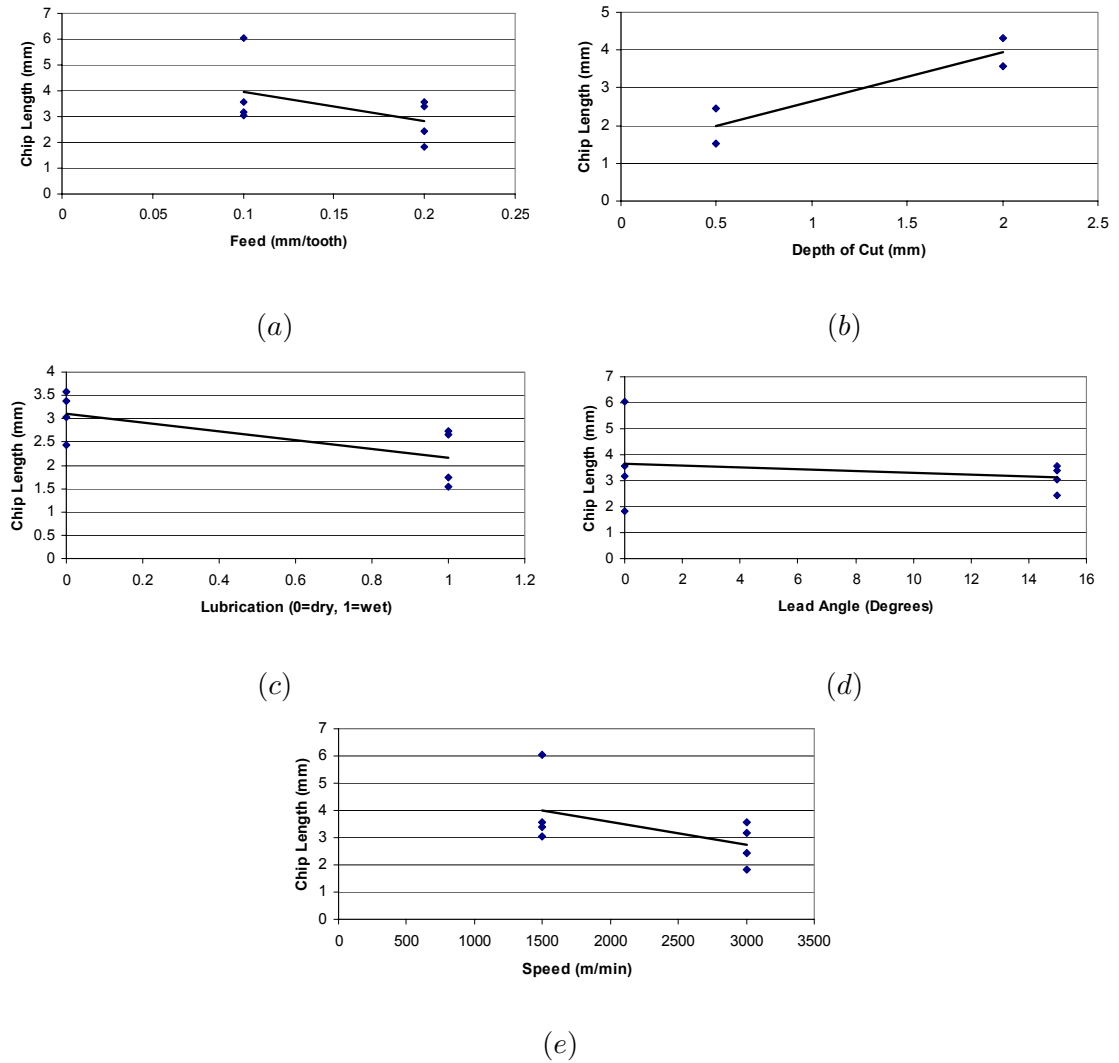
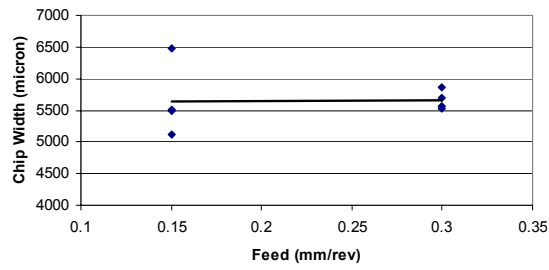


Figure A.11: Effect of process parameters on the chip length for milling: (a) feed (b) depth of cut (c) lubrication (d) lead angle (e) speed.

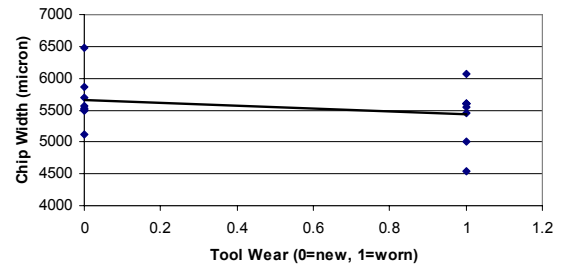
Appendix B

Graphs of Drilling Correlations & Effects

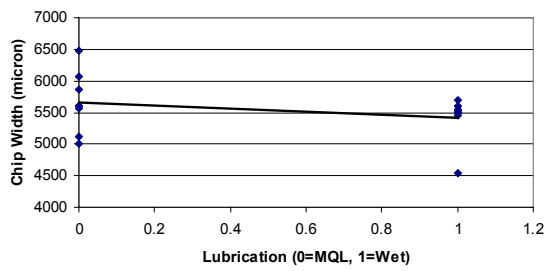
Each diamond on a graph represents the numerical (rather than weight) averaged output of all the chips from one experiment.



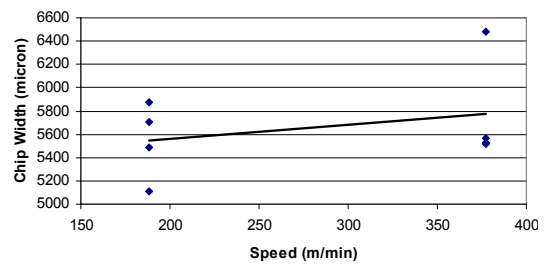
(a)



(b)

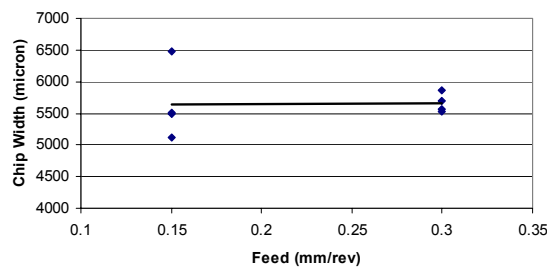


(c)

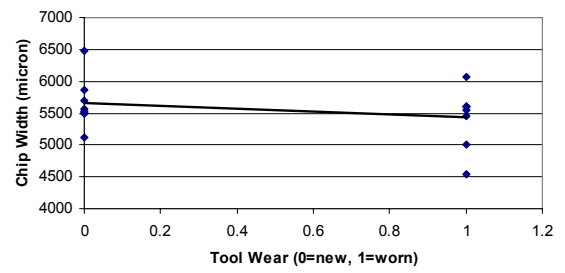


(d)

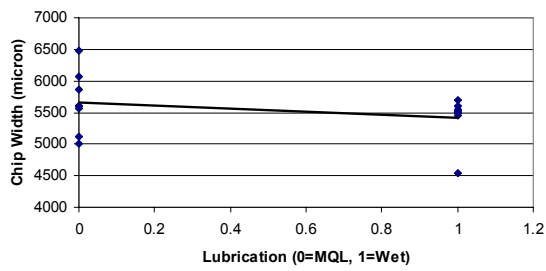
Figure B.1: Effect of process parameters on the chip width for drilling: (a) feed (b) tool wear (c) lubrication (d) speed.



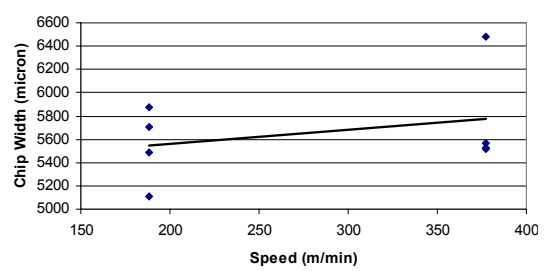
(a)



(b)



(c)



(d)

Figure B.2: Effect of process parameters on the chip width for drilling: (a) feed (b) tool wear (c) lubrication (d) speed.

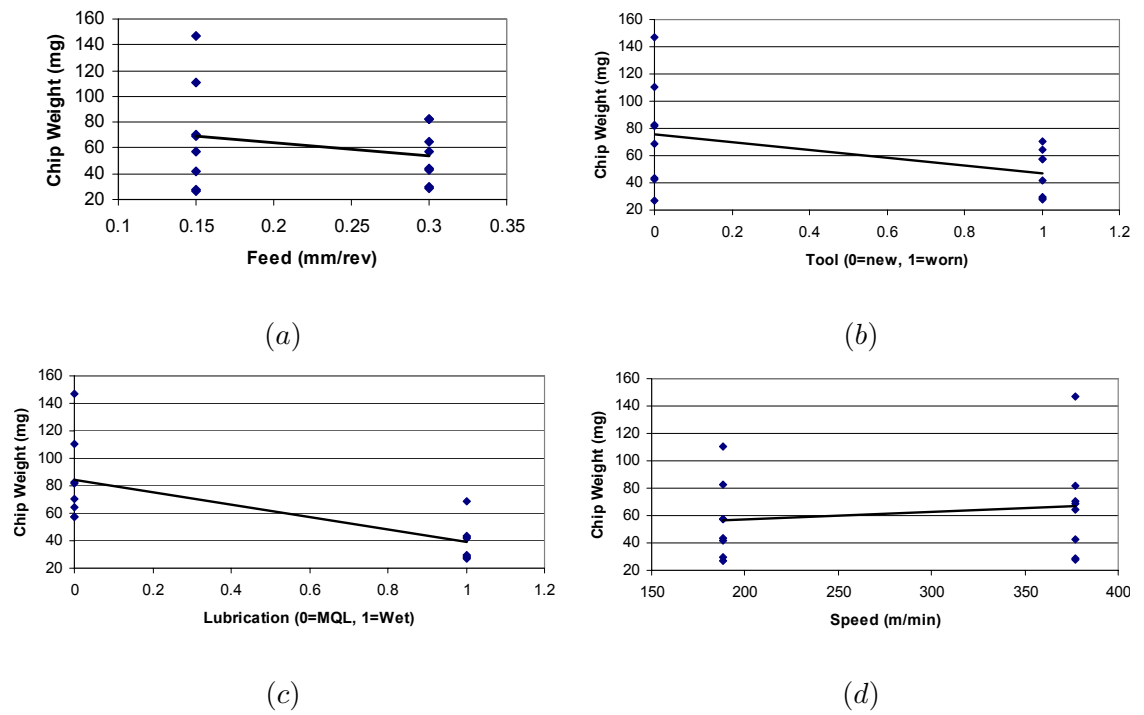
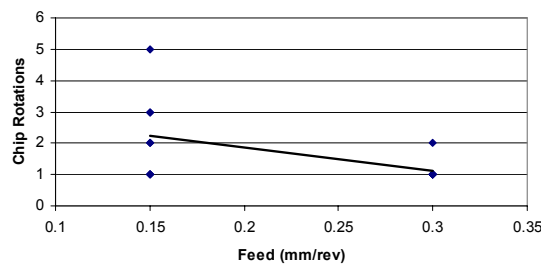
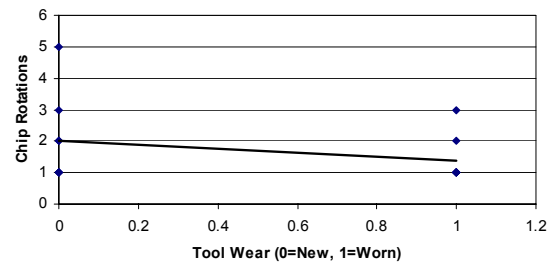


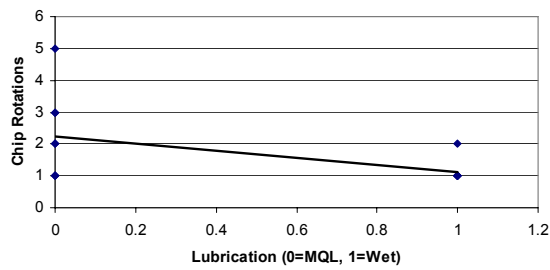
Figure B.3: Effect of process parameters on the chip weight for drilling: (a) feed (b) tool wear (c) lubrication (d) speed.



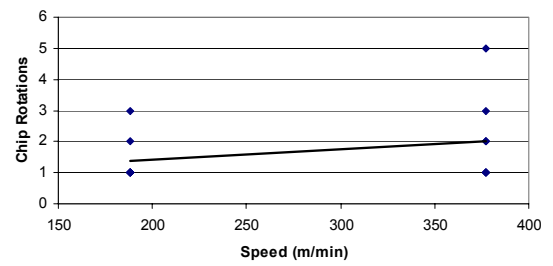
(a)



(b)

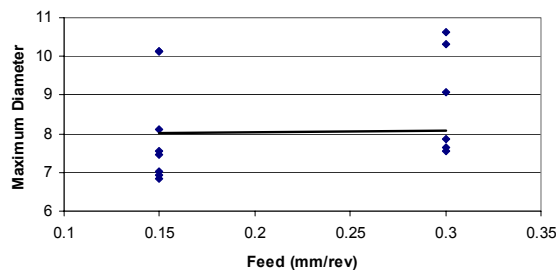


(c)

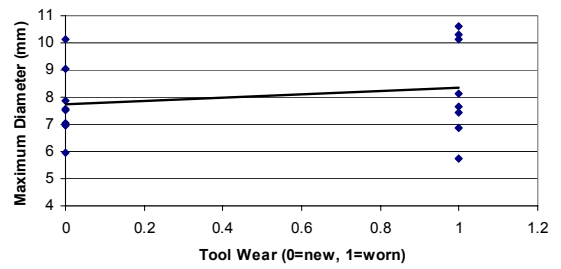


(d)

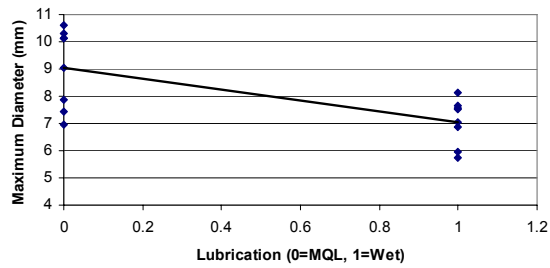
Figure B.4: Effect of process parameters on the chip rotations for drilling: (a) feed (b) tool wear (c) lubrication (d) speed.



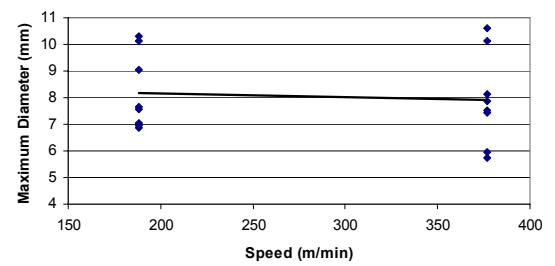
(a)



(b)

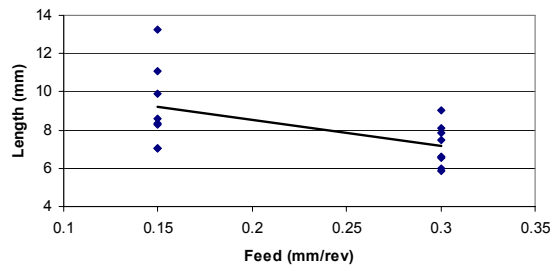


(c)

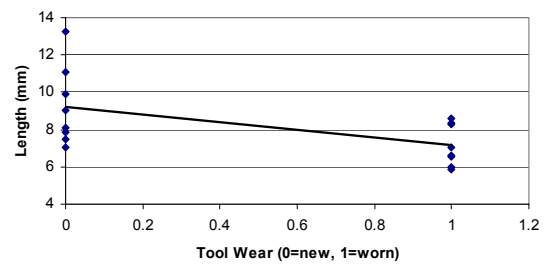


(d)

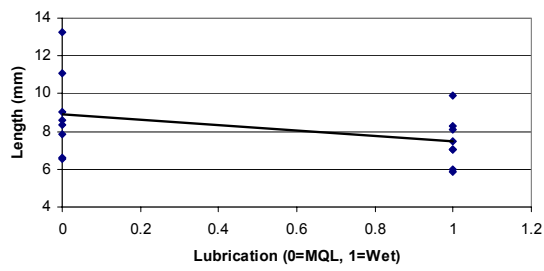
Figure B.5: Effect of process parameters on the chip maximum diameter for drilling: (a) feed (b) tool wear (c) lubrication (d) speed.



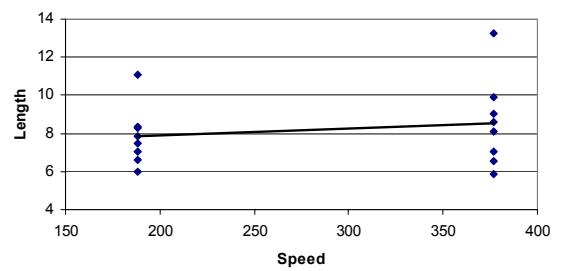
(a)



(b)



(c)



(d)

Figure B.6: Effect of process parameters on the chip maximum diameter for drilling: (a) feed (b) tool wear (c) lubrication (d) speed.

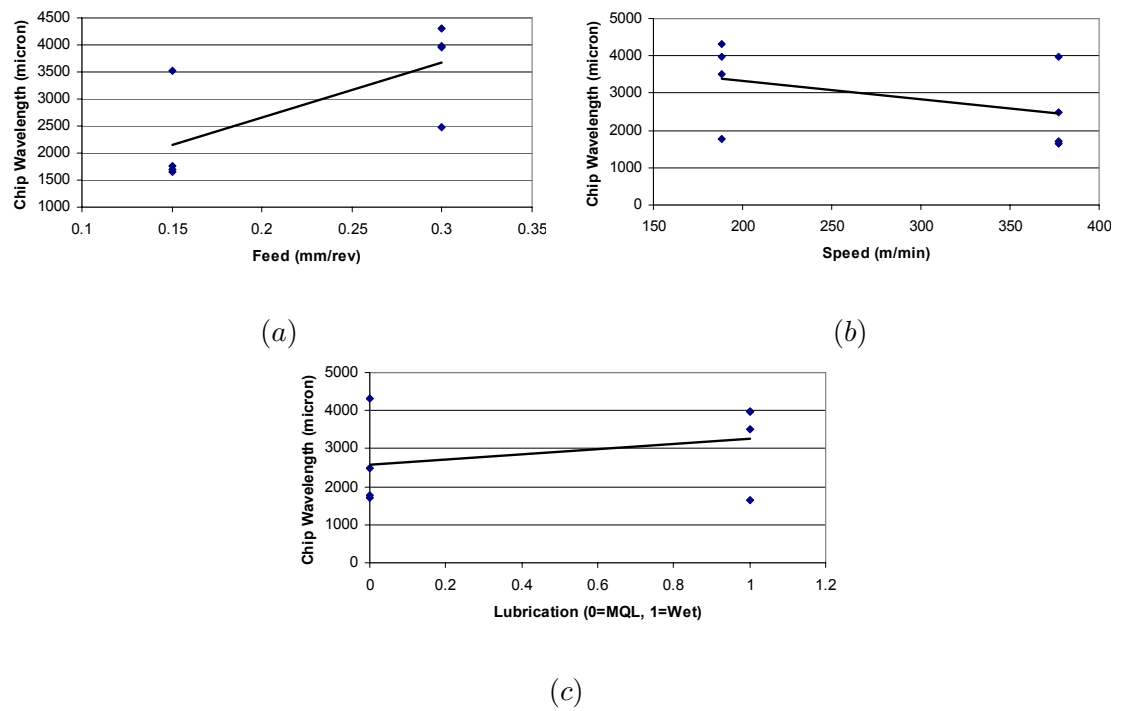
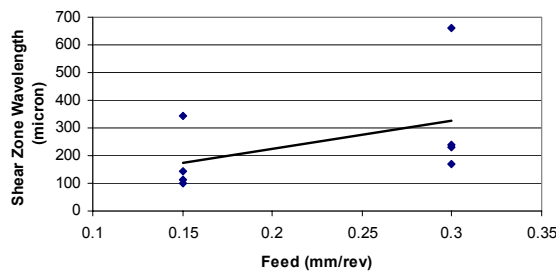
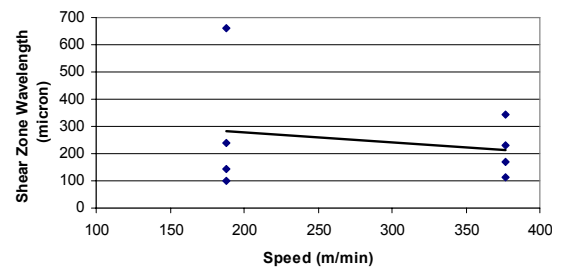


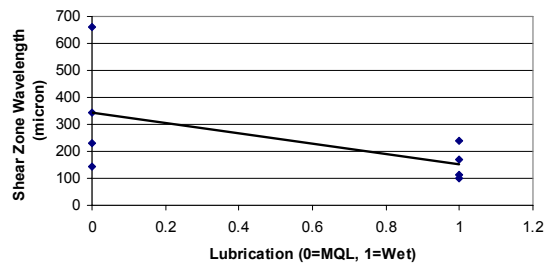
Figure B.7: Effect of process parameters on the chip wavelength for drilling: (a) feed (b) speed (c) lubrication.



(a)



(b)



(c)

Figure B.8: Effect of process parameters on the chip shear zone wavelength for drilling: (a) feed (b) speed (c) lubrication.

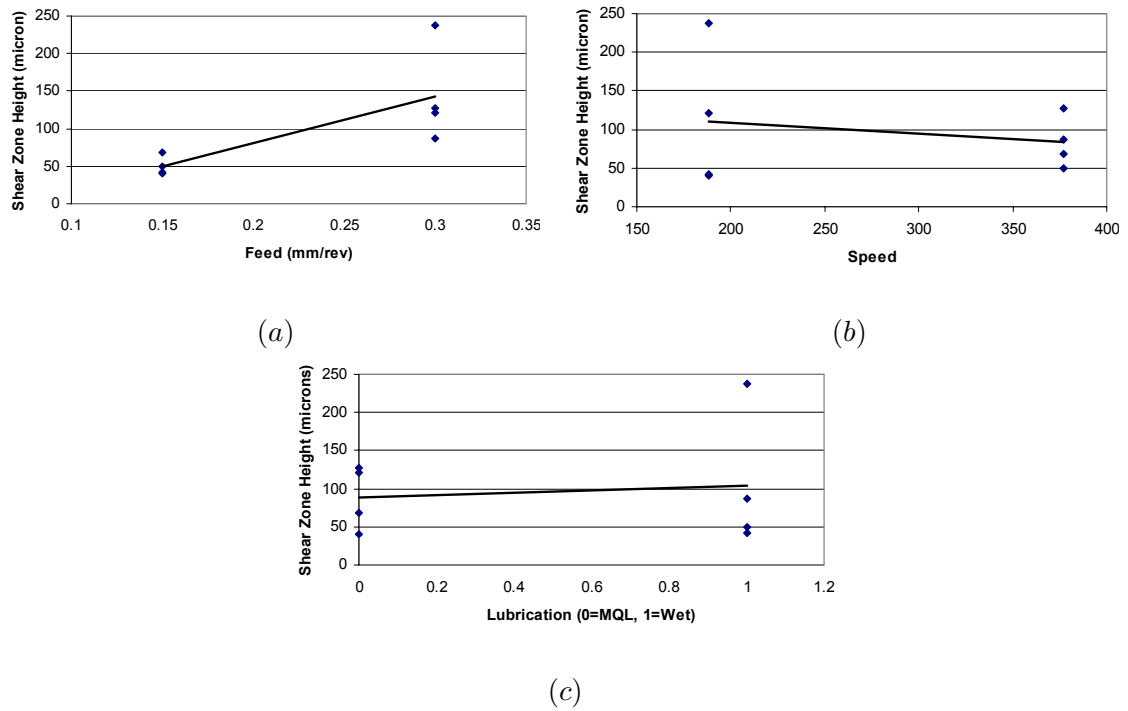


Figure B.9: Effect of process parameters on the chip shear zone height for drilling: (a) feed (b) speed (c) lubrication.

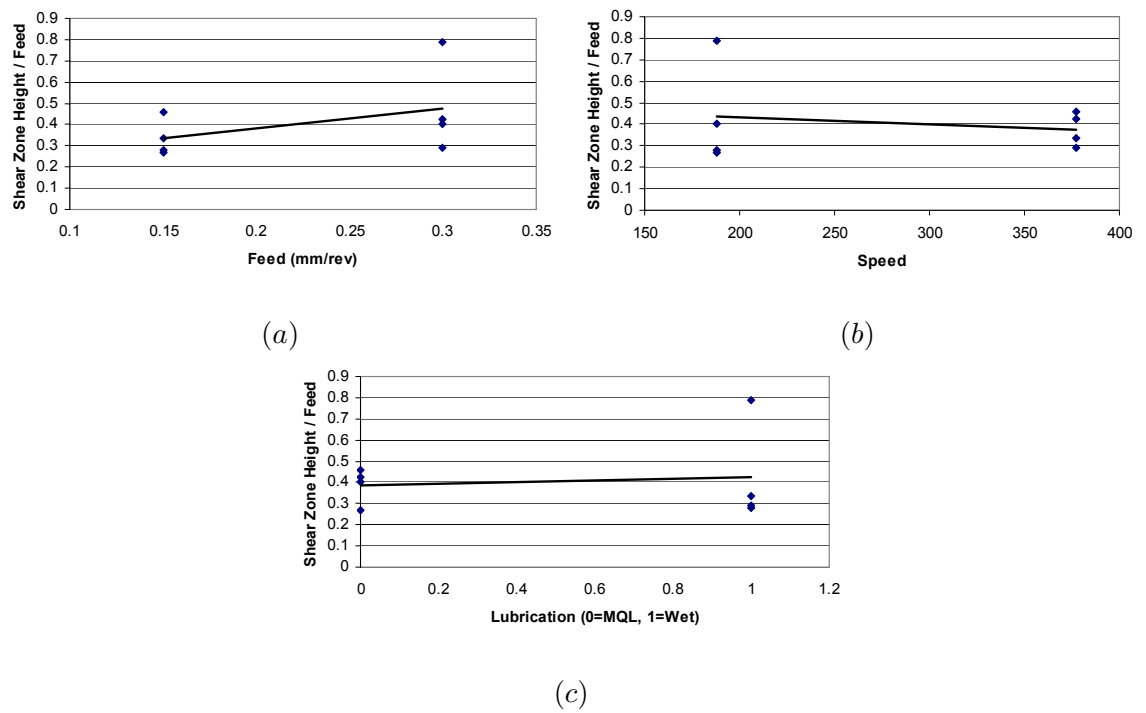


Figure B.10: Effect of process parameters on the chip shear zone height divided by the feed for drilling: (a) feed (b) speed (c) lubrication.